Journal of Petroleum Science and Engineering 186 (2020) 106691

Contents lists available at ScienceDirect

Journal of Petroleum Science and Engineering

journal homepage: http://www.elsevier.com/locate/petrol

Water flooding of oil reservoirs: Effect of oil viscosity and injection velocity on the interplay between capillary and viscous forces

Danial Arab *, Apostolos Kantzas, Steven L. Bryant

Department of Chemical and Petroleum Engineering, University of Calgary, 2500 University Drive NW, Calgary, AB, T2N 1N4, Canada

ARTICLE INFO

Keywords:
Unconventional heavy oil
Conventional light oil
Water flooding
Instability analysis
Viscous fingering

ABSTRACT

Water flooding is the most widely applied recovery process in both conventional and heavy oil reservoirs. It is generally accepted that theories explaining water flooding performance in light oil reservoirs are not applicable to heavy oil reservoirs. Nonetheless, there is a lack of a systematic study discussing the underlying mechanisms of water flooding in heavy oil systems. This article presents findings of water flooding experiments and discusses the interplay between viscous and capillary forces as a function of oil viscosity and injection velocity. Experimental data of 178 core floods were used to develop a new dimensionless capillary number, $N_{Ca} = \left(\frac{\mu_w V_w}{\sigma \, Cos\theta\varphi}\right)^{0.26}\left(\frac{\mu_w}{\mu_o}\right)^{0.50}\left(\frac{K}{LD}\right)^{0.18}$, which is useful in predicting water flood performance for a wide range of oil to water viscosity ratio up to 15,000. This scaling parameter along with the Peters and Flock's (Peters and Flock, 1981) instability number were used to map the interplay between capillary and viscous forces. It was found that there is a critical oil to water viscosity ratio (≤20) below which the flow is stable (having instability numbers below a critical value) and viscous-dominant. In these cases, breakthrough oil recovery monotonically increases with increasing injection velocity. For viscous oils with viscosity of greater than 160 mPa s, flow is identified as pseudo-stable flow with instability numbers above a critical instability number. In these cases, breakthrough oil recovery is almost independent of injection velocity. In intermediate oil to water viscosity ratio of 20–160, breakthrough oil recovery increases with decreasing injection velocity, suggesting the flow regime is capillary-dominant. In these cases, imbibition activated at slower velocities has been identified as the main mechanism responsible for incremental oil recovery. In viscous oil systems ($160 < \mu_o < 15{,}000$), late time oil recovery monotonically increases with decreasing injection velocity. This increase in oil recovery is more pronounced in more viscous oil systems suggesting the importance of capillary forces in these systems. Results of this study suggest some new insights on the mechanisms of water flooding as a cost effective non-thermal EOR technique and how this can be very different in light oil systems compared to heavy oil reservoirs.

1. Introduction

Unconventional oils have been recognized as extensive resources to supply increasing global energy demand, specifically with increasing decline in conventional oil reserves. Development of these resources is very challenging since they are either very viscous, such as oil shales or heavy oils, or not permeable such as tight oil or gas, gas shales, and coalbed methane reservoirs (Holditch, 2013). Heavy oil and oil sand deposits in western Canada have been estimated as 1.7 10^{12} barrels, which is one of the largest unconventional resources in the world (Alberta Energy and Utilities Board, 2001). Heavy oil reservoirs in Alberta and Saskatchewan are very viscous, with viscosity in the range of 50 to 50,000 mPa s (cP) at reservoir temperature and pressure, and so their primary production has been reported as low as 5% original oil in place (OOIP) through solution gas drive mechanism (Bryan and Kantzas, 2008). The remaining oil in place is an immense target for improved oil recovery methods. Many of these reservoirs are either too small or thin, which makes them poor candidates for thermal recovery processes

* Corresponding author.
E-mail addresses: danial.arab@ucalgary.ca (D. Arab), akantzas@ucalgary.ca (A. Kantzas), Steven.Bryant@ucalgary.ca (S.L. Bryant).

https://doi.org/10.1016/j.petrol.2019.106691
Received 9 September 2019; Received in revised form 5 November 2019; Accepted 12 November 2019
Available online 16 November 2019

where heat loss to overburden and underburden formations should be minimized (Farouq Ali, 2006; Luo et al., 2007). Therefore, non-thermal/cold recovery techniques have been suggested as alternatives to thermal processes to develop these reservoirs.

Water flooding is the most widely applied enhanced oil recovery (EOR) method in both conventional and unconventional oil reservoirs (Willhite, 1986). In this process, water is injected into the reservoir through an injection well to displace oil in front of it towards the production well. In heavy oil reservoirs, water flooding is often the first process to apply either along with primary production to maintain reservoir pressure or after primary recovery to displace oil. Before the first appearance of water in the production well, defined as water breakthrough, only oil is moving in the reservoir delivering 100% oil cut in production well, assuming that initial water is at its irreducible (immobile) saturation. After water breakthrough, both oil and water flow based on their relative permeabilities leading to a decrease in oil cut and increase in water cut in production wells up to a stage where practical residual oil saturation to water flood is achieved. At this stage water flooding becomes uneconomical and reservoir will be considered for different EOR methods to produce the residual oil left in the reservoir.

In conventional light oil water flooding theory, the viscosity ratio between oil and water is assumed to be 1. This assumption is not valid in heavy oil reservoirs where the viscosity ratio between oil and water could be up to 50,000 (Mai and Kantzas, 2009). Therefore, oil mobility ($\frac{K_o}{\mu_o}$) is much lower than that of water ($\frac{K_w}{\mu_w}$) in heavy oil reservoirs leading to an early water breakthrough, called unstable displacement in water flooding or viscous fingering phenomenon. This viscous fingering phenomenon has been reported in any wettability conditions and increases the duration of simultaneous flow of oil and water (Craig, 1971; Buckley and Leverett, 1942). This unstable displacement in water flooding of heavy oil reservoirs is attempted to be quantified through instability

Table 1
Summary of literature discussing water flooding in heavy oil systems.

Heavy oil characteristics		Porous medium characteristics		Core flood characteristics						Reference
μ (mPa.s)[a]	d (kg/m³)[a]	Sand type	Sand grain size (μm)	K (d)	φ (%)	OOIP (% PV)	V (ft/d)	Lc (cm)	Dc (cm)	
11,500	981.5	Lane Mountain 70	150–250	14	46	N/M[b]	0.07, 1.40	9.30	2.54	Mai et al. (2007)
6500 11,500	970 981.7	Lane Mountain 70	58 217	0.80–9.00	35.50–46.40	88.40–95.04	0.07, 1.31	16.70–53.20	2.60 3.63 3.81	Mai and Kantzas (2008)
4,650, 11,500	980, 981.5	Lane Mountain 70	N/M[b]	1.86–2.80	35.50–37.2	88.40–89.67	0.07, 0.35, 0.69, 1.04, 1.38	16.50–17.55	3.81	Mai and Kantzas (2009)
11,500	981.7	Lane Mountain 70	150–180	3.86, 10	34.80–46.00	91.90	0.01–0.03	9.3, 114.8	2.54, 8.89	Mai (2008),
10.20, 10.40, 10.60, 11, 19, 46.70, 95, 110, 112 (Non-polar mineral oil)	N/M[b]	Silica sand	74–105	3.65	34.80	91–95	0.001–0.01	46.6	5.64	Sarma et al. (1990)
430, 1,088, 1,450, 1,860, 5,410, 13,550	N/M[b]	Ottawa sand	149–250	6.50–7.10	35.60–36.00	89.5–96.2	0.32–0.56	14.2	4.25	Wang et al. (2006)
18, 408.3	886, 941.3	Ottawa sand	127–177	9.20, 17.80	33.80, 38.70	84.6–91.7	0.01–47.60	60, 100	5.04	Symonds et al. (1991)
4435	1001	Quartz sand	95–840	9.30–9.89	34.42–36.65	85.22–91.17	4.66	60	2.54	Lu et al. (2016) [c]
102.5	N/M[b]	Ottawa sand	127–177	18	38	90	0.11–47.88	23	4.8	Peters and Flock (1981)
60, 560, 1,440, 5,200, 10,500 (Mineral oils)	N/M[b]	Boise sandstone core	N/M[b]	6	29	83–91.1	0.05, 0.2, 1	30.48	5.08	Doorwar and Mohanty (2017)
3.5, 72, 80, 120, 250, 1,050, 1,111, 1,230, 1290	N/M[b]	Ottawa sand (F-95), reservoir sand	57.50	0.23–7.90	23–39	65–89	1, 3.30, 5, 13, 14	30.48	3.81, 5.08	Koh et al. (2018)
0.95, 105.36, 310.53	782.3, 966.7, 879.9	Ottawa sand	127–177	18.5	38	84.74–91.40	0.11, 0.44, 0.87, 2.18, 4.35, 6.96, 8.70, 10.44, 20.89, 34.81, 48.74	22.80, 22.90, 23.60, 23.70, 110.5, 112.8, 115.9, 116.1	4.84, 4.97	Peters (1979)
105.4	966.7	Ottawa silica sand	127–177	14–19	36	89	0.09, 0.57, 2.86, 7.75, 28.58, 114.31[d]	23, 53, 110	2.4, 4.8	Demetre et al. (1982)
405 (Non-polar mineral oil)	877	Ottawa sand	74–105	3.6	35	93–96	0.66, 1.31, 2.63, 5.27, 10.55	46.7	5.64	Maini et al. (1990)

[a] At ambient temperature.
[b] N/M: Not mentioned.
[c] These core flood experiments were done at reservoir temperature (54 °C).
[d] Injection velocities in this study have not been reported and so, we calculated them back from the instability numbers.

analysis, which will be discussed later. In addition, since the available area for flow of oil and water is very different in heavy oil systems compared to conventional light oil reservoirs relative permeability concepts may be completely different (Mai and Kantzas, 2009). These complexities make it impossible to simply apply the theories explaining water flooding in conventional light oil reservoirs to the heavy oil systems (Emadi and Sohrabi, 2012).

The combination of viscous and capillary forces is responsible for oil recovery at any given injection velocity. Some studies reported an increase in oil recovery with increasing injection velocities support the importance of viscous forces, strengthen with increasing velocity, over the capillary forces. On the other hand, the other studies reported a better oil recovery at slower injection velocities attribute this incremental oil recovery to the imbibition process, which is a time-dependent slow process. There are numerous systematic studies discussing the effect of governing parameters on water flooding of light oil reservoirs. However, there is only a few studies investigating the effect of these parameters on the performance of water flooding in heavy oil systems. Table 1 summarizes the experimental studies on water flooding in viscous oil systems. The literature presented in Table 1 discuss water flooding in water-wet systems. A few of these studies quantified the degree of water-wetness through reporting contact angle such as Wang et al. (2006), who reported contact angle of near zero and Moore and Slobod (1955) who reported contact angle of 30, 37, and 41°, while most of the cited literature (Mai and Kantzas, 2008; Mai et al., 2007; Maini et al., 1990; Sarma et al., 1990; Symonds et al., 1991; Lu et al., 2016; Doorwar and Mohanty, 2017; Koh et al., 2018) just qualitatively reported that the cores were strongly water-wet. As can be inferred from Table 1, each work was done with a limited range of oil viscosities with specific experimental settings in terms of core permeability, porosity, length, diameter, original oil in place, and velocity. These variabilities may make it impossible to compare these works with each other to understand the effect of governing parameters on water flooding. The current research was aimed to give some insights on the balance between capillary and viscous forces as a function of oil viscosity and injection velocity within one experimental setting.

2. Background

2.1. Balance of imbibition and viscous forces

In water-wet rocks water imbibes into small to medium-sized pores through capillary forces, enhanced with increasing rock water-wetness, pushing oil out into the large pores where oil can easily flow (Anderson, 1987). An oil bank is created ahead of the frontal zone where both oil and water flow leaving residual oil behind as discontinuous ganglia in the center of the larger pores (Moore and Slobod, 1955). This discontinuous residual oil is almost immobile; therefore, no or very little oil is produced after water breakthrough in strongly water-wet systems (Craig, 1971). In these systems, oil recovery is increased with increasing the degree of rock water-wetness. This oil recovery behavior has been suggested for conventional light oils where no viscous fingering occurs. On the other hand, there are some authors arguing that the maximum oil recovery can be achieved at wettability conditions towards intermediate wet, where oil and water have the same chance to imbibe into the pores with the minimum amount of oil trapped by capillary forces (Buckley et al., 1996; Kennedy et al., 1955; Jadhunandan and Morrow, 1995; Moore and Slobod, 1955; Morrow, 1990; Morrow et al., 1986, 1994, 1998; Owolabi and Watson, 1993; Rao et al., 1992a, 1992b; Rathmell et al., 1973; Salathiel, 1973; Skauge et al., 2006; Wardlaw, 1980,1982; Wardlaw, 1992; Zhou et al., 2000). These studies suggest that in a strongly water-wet system, oil is possibly bypassed in the larger pores since the water imbibes only into the smaller pores (Moore and Slobod, 1955). In addition, oil entrapment due to “snap off” is occurred in a strongly water-wet system with the maximum interfacial forces tending to disconnect the oil (Anderson, 1987).

In heavy oil systems, although the general belief is that viscous forces are dominant in water flood recovery compared to capillary forces, there are some articles addressing the importance of imbibition in heavy oil systems (Emadi and Sohrabi, 2012; Lu et al., 2016; Mai and Kantzas, 2009; Smith, 1992). Fig. 1a shows that oil recovery increases as the flood velocity decreases, suggesting a detrimental effect of viscous forces on oil recovery (Mai and Kantzas, 2009). All the studies whose results are presented in Fig. 1a and b were done with water-wet sands. These improvements in heavy oil recovery after water breakthrough, when at least one low resistance water channel is already created leading to low pressure gradient across the system, suggest that capillary forces are of importance in heavy oil systems. Although there is an unfavorable mobility ratio in all the studies presented in Fig. 1a leading to unstable displacement, capillary forces enhanced at slower velocities are recognized as the main mechanism to recover heavy oil (Mai and Kantzas, 2009; Mei et al., 2012). With flooding at a slower velocity there is more time for water to transversely imbibe into the small pores to push oil out rather than just being circulated along the flow direction, which is a case in high velocity water floods. Kantzas and Brook also reported that gentle floods deliver better oil recovery (Kantzas and Brook, 2004). In another study, Doorwar and Mohanty investigated an unstable immiscible flow during displacement of viscous oils (mineral oils of different viscosities: 60, 560, 1,440, 5,200, 10,500 mPa s) by water (Doorwar and Mohanty, 2017). They performed eight core flood experiments where one single water-wet Boise sandstone core was used in all the experiments. After each experiment, the core was cleaned by flushing with toluene and acetone and reused in the next experiment. Their results show that with increasing oil viscosity water breakthroughs faster leading to a lower oil recovery, as expected. In addition, at the same oil to water viscosity ratio (10,500) decreasing injection rate delays water breakthrough leading to incremental oil recovery, as suggested by previous investigators (Mai and Kantzas, 2009). The imbibition phenomenon in unstable displacements has been seen like imbibition in naturally fracture reservoirs in a way that fingers act like a fracture from which water imbibes into the un-swept regions of the reservoir which resemble matrix blocks (Smith, 1992). However, it seems that there is an intermediate injection velocity at which breakthrough recovery is maximized (Fig. 1b). This intermediate velocity seems to be high enough to enhance viscous forces and at the same time low enough to take advantage of capillary forces to maximize heavy oil recovery in unstable displacement floods.

The local maxima in Fig. 1b attributed to the capillary outlet end effect (Maini et al., 1990). Although capillary end effects are not important on a reservoir scale, they may remarkably affect core flood results in terms of oil recovery and saturation profiles on a lab scale (Anderson, 1987). Capillary outlet end effect has been defined as accumulation of the wetting phase at the core outlet, where the wetting phase tend not to leave the capillaries and produce. In water flooding of a water-wet core, capillary outlet end effect causes a delay in water breakthrough time. On the other hand, in water flooding of an oil-wet core capillary outlet end effect has no effect on water breakthrough time. Capillary outlet end effect is more pronounced at low injection velocities, where capillary pressure takes over in spreading of the displacement front (Anderson, 1987) retarding the wetting phase breakthrough. Capillary outlet end effect results in a lower breakthrough oil recovery in oil-wet cores (Anderson, 1987), while in water-wet cores this effect is a function of oil viscosity and the balance between capillary outlet and inlet end effect. Capillary inlet end effect is only reported in strongly water-wet cores and is due to spontaneous localized imbibition of water upon its first contact with rock accompanying with a counter flow of oil (Anderson, 1987; Kyte and Rapoport, 1958). At late times during the flood, water tends to pass only through the localized areas developing a non-linear flow within the core. This effect can be considered as capillary-driven fingering, which is less pronounced at low oil to water viscosity ratio and low injection velocities. At low injection velocities, capillary pressure has more effect to

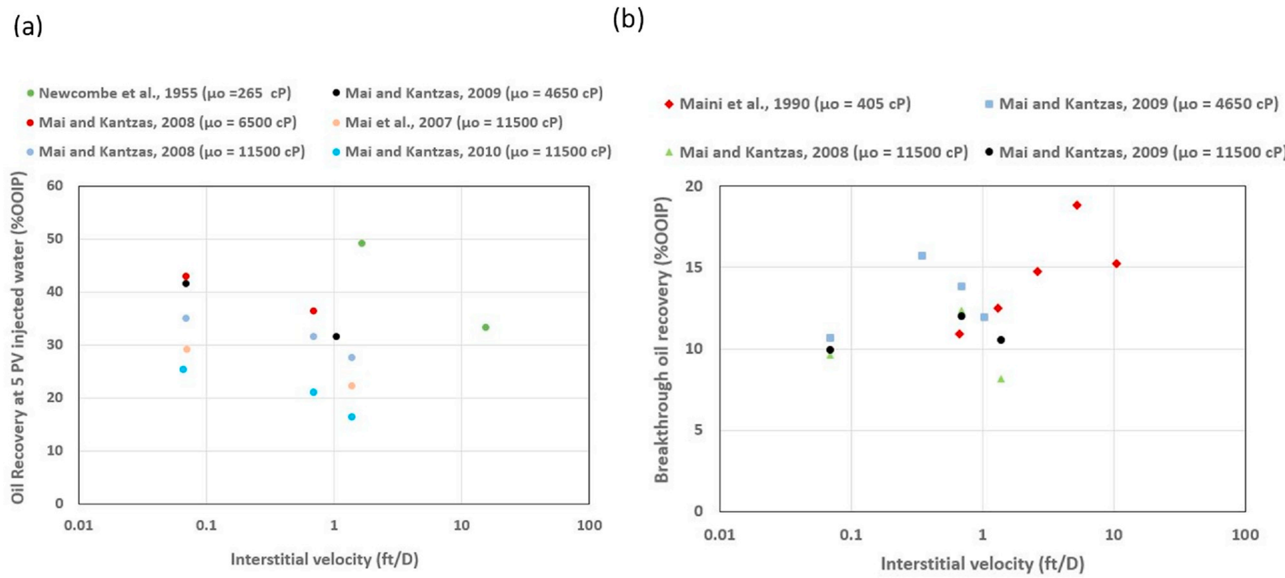

Fig. 1. Oil recovery as a function of interstitial velocity a) after 5 PVI b) at breakthrough.

redistribute water across the entire across sectional area of the core in the inlet, minimizing the inlet end effect (Kyte and Rapoport, 1958). Capillary inlet end effect is reported to cause a decrease only in breakthrough oil recovery with no significant effect on ultimate oil recovery (Anderson, 1987). Therefore, core flood experiments, specifically with water-wet cores, should be done at an optimum velocity which is high enough to minimize the capillary outlet end effect and at the same time low enough to avoid the capillary inlet end effect. In addition to the velocity, the core length should be long enough to minimize the effect of capillary end effects (Anderson, 1987). To meet these conditions, Rapoport and Leas (1953) defined the scaling coefficient of $1 \leq LV\mu_w$, where L, V, and μ_w are core length in cm, injection velocity in cm/min, and water viscosity in mPa.s, respectively. Rapoport and Leas (1953) did not provide any upper limit for the above scaling coefficient; however, some other literature (Anderson, 1987; Batycky et al., 1981) citing the Rapoport and Leas's (1953) reported the upper limit of 5 for the scaling coefficient (i.e., $1 \leq LV\mu_w \leq 5$). These later works may indicate that the scaling coefficient should be optimum rather than being a maximum, to make sure that there is no capillary inlet end effect. Literature data were replotted against the mentioned scaling coefficient for both light and viscous oils (Fig. 2). For light oil water floods (Fig. 2a), the flood is mostly stabilized beyond scaling coefficient equal to 1, i.e., no further increase in oil recovery with further increasing the scaling coefficient meaning the capillary outlet end effect is properly dealt with. However, for the floods done with more viscous oils (Fig. 2b), the initial increase in oil recovery with increasing the scaling coefficient suggests proper dealing with capillary outlet end effect, likewise light oil cases. However, in all the data sets presented in Fig. 2b there is a final decrease in oil recovery with a further increase in scaling coefficient which suggests that the floods are not stabilized which may be due to either capillary inlet end effect (capillary-driven fingering) or unstable flood and viscous fingering, which will be discussed later.

By comparing the discussed literature, it seems that the effect of injection velocity on oil recovery is also dependent on oil viscosity; however, there is not a systematic study with one single experimental setting to study these effects in light oil vs. viscous oil systems.

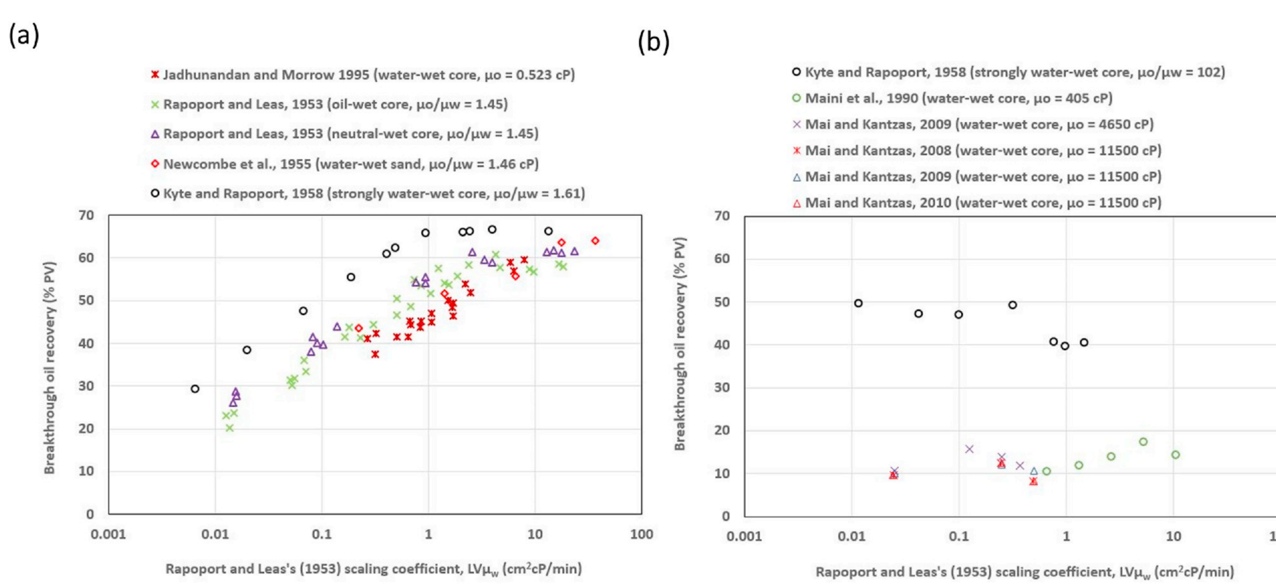

Fig. 2. Breakthrough oil recovery versus Rapoport and Leas's (1953) scaling coefficient for a) light oil b) viscous oil systems.

3. Materials and methods

3.1. Materials

Milli-Q apparatus was used to purify water (18.2 MΩ cm at 25 °C, pH – 6.5), which was used in all the experiments. Dodecane (reagent grade, ≥ 99%, Sigma-Aldrich), mineral oil # 1 (model # 5011, Drakeol, Fluke, Hart Scientific), mineral oil # 2 (light mineral oil, NF/FCC, Fisher Scientific), mineral oil # 3 (heavy mineral oil, USP/FCC, Fisher Scientific), mineral oil # 4 (rotational viscosity standard, RTM21, Sigma-Aldrich) were used as received. In addition, two different heavy crude oils from western Canada were used. Water cut in heavy oil samples were analyzed through nuclear magnetic resonance (NMR) technique, which was less than 0.5 wt %. Table 2 summarizes properties of different oils used in this study.

A Brookfield viscometer (DV2T Pro Extra Viscometer) was used to measure oil viscosity. The Wilhelmy plate technique (Dynamic Contact Angle Meter and Tensiometer, Dataphysics) was utilized to measure interfacial tension (IFT) between different oils and deionized water (DIW). The measured IFT between DIW and dodecane is 51.5 mN/m, which is in good agreement with literature (Rodriguez et al., 2016; Zeppieri et al., 2001). In all the sand-pack flooding experiments, water-wet (with contact angle of 32°) silica sands (50–70 mesh (210–297 μm), Sigma-Aldrich) were used.

3.2. Experimental procedure

To begin the core flooding experiments, silica sands were packed into a 30.7 cm long steel tube with an internal diameter of 1.6 cm. The packed bed was vacuumed for 30 min and then saturated with DIW. Bed porosity was measured through weight measurements before and after saturation step. Permeability to water was then measured through injecting water at different velocities and applying Darcy's law. The bed pore volume, permeability, and porosity of different packs were in the range of 22.21 ± 0.11 mL, 38.79 ± 1.85 Darcy, and 37.15 ± 0.18%, respectively. Afterwards, oil was injected into the DIW saturated core to reach an irreducible water saturation i.e., no water production was observed. The core was then water flooded, and effluents were collected using a fraction collector. An in-line densitometer (Paar DMA HPM), equipped with a water bath to control temperature of the densitometer cell, was used downstream the core holder to precisely measure the effluents' density. The schematic of the core flooding experimental set-up is depicted in Fig. 3. The real time density data allows precise calculation of breakthrough time. Temperature of the densitometer cell was set equal to 25 °C during the whole core flooding experiments. A toluene separation technique was applied to precisely measure oil cut in effluents in the floods done with heavy oils. In experiments with mineral oils, oil and water were completely separated in the effluents allowing calculations of oil and water cuts by volume measurement. The Dean Stark technique was also applied to double check final oil recovery. The difference between final recoveries obtained by toluene separation technique and the values based on the Dean Stark method was less than 0.5%.

Table 2
Properties of different oils used in this study.

Oil type	Density (kg/m^3) at 25 °C	Viscosity (mPa.s) at 25 °C	IFT (mN/m)
Dodecane	750.0	1.7	51.5
Mineral oil # 1	874.1	21.4	31.0
Mineral oil # 2	860.0	53.7	31.2
Mineral oil # 3	830.0	157.4	33.7
Mineral oil # 4	893.5	494.0	44.6
Heavy oil # 1	976.4	1012.0	65.8
Heavy oil # 2	980.0	14,850.0	59.0

4. Results and discussion

4.1. Coreflooding experiments

Nineteen Coreflooding experiments were designed to study the interplay between capillary and viscous forces (Table 3). In these experiments, the effect of oil viscosity and injection velocity, as governing parameters suggested by capillary number concept, on the performance of water flooding was investigated. These corefloods were conducted at seven different oil to water viscosity ratios and two different injection velocities of 0.7 and 24.3 ft/D (2.5×10^{-6} m/s and 8.6×10^{-5} m/s). To further understand the water flooding behavior in light oil systems, three additional core flooding experiments with 0.1, 121.5, and 243 ft/D (3.5×10^{-7}, 4.3×10^{-4}, and 8.6×10^{-4} m/s, respectively) were performed with dodecane as the oil phase. The injection rate was varied in experiments 10 and 50 to study the effect of step-wise changing of injection velocity on the flood performances. The size of sand used in different experiments was the same, based on which pore throat radius was estimated as 28.70 ± 0.66 μm using the bundle of capillary tube model (Lake et al., 2014). A sample of an in-line densitometer data is presented in Fig. 4.

As shown in Fig. 4b, only oil (dodecane in this case) with density of 0.77 gr/cm^3 is produced up to 0.5 pore volume injected (PVI), when the first drop of water passes through the densitometer cell resulting in a sharp increase in the effluent density. Beyond breakthrough, density profile reflects the oil and water cuts in the effluents. As shown in Fig. 4a, beyond 2.5 PVI water cut is 100% with zero oil production, which is consistent with water flooding behavior of light oils in water-wet systems. The density data was used to precisely determine breakthrough time in all the experiments. This technique to measure water breakthrough time in core flooding experiments was first introduced by Olsen (2018), which is specifically important in heavy oil cases where determination of breakthrough time is very challenging. In heavy oil water floods, water breaks through very early when oil production is small making determination of breakthrough time through slope of the recovery curve very challenging. In these systems, due to similar density of heavy oil and water and also high oil viscosity visual identification of the point of water breakthrough is difficult (Mai and Kantzas, 2009); therefore, breakthrough time is conventionally inferred from the pressure gradient profile, which keeps increasing in constant rate floods up to the breakthrough point beyond which pressure gradient across the core declines sharply. The point of pressure decline indicates formation of at least one finger of low resistance through which water passes.

Oil recovery vs. pore volume injected of water for different oils at different velocities is plotted in Fig. 5. As expected, for both 0.7 and 24.3 ft/D floods oil recovery is decreased with increasing oil viscosity. To better understand the effect of injection velocity for each oil, oil recovery vs. PVI for each oil at different velocity is plotted in Fig. 6. The results presented in Fig. 6 suggest that the higher velocity floods (24.3 ft/D) deliver more oil than that of lower velocity floods (0.7 ft/D) when the oil viscosity is lower than 53.7 mPa s (i.e., in Fig. 6a, b, and c). These observations suggest that for this range of oil viscosity viscous forces, enhanced by increasing injection velocity, are the dominant driving mechanism for oil recovery. On the other hand, the opposite behavior was observed for higher oil viscosities where oil recovery decrease with increasing injection velocity (Fig. 6d, e, f, and g). These results suggest that for this range of oil viscosity (higher than 53.7 mPa s) capillary forces, enhanced at slower velocity floods, are the main driving force for oil recovery. At low oil viscosity, there is less chance for water to finger through the oil to make a flood unstable. This viscous fingering would be more likely to happen at higher velocity floods, which will be discussed later. In case of high oil viscosity, decreasing injection velocity resulting in less severe viscous fingering will provide a more chance for water to imbibe into the small and medium sized pores to push the oil out, rather than just being circulated through the water channels which is the case in high velocity floods. So more stable flood with less viscous fingering

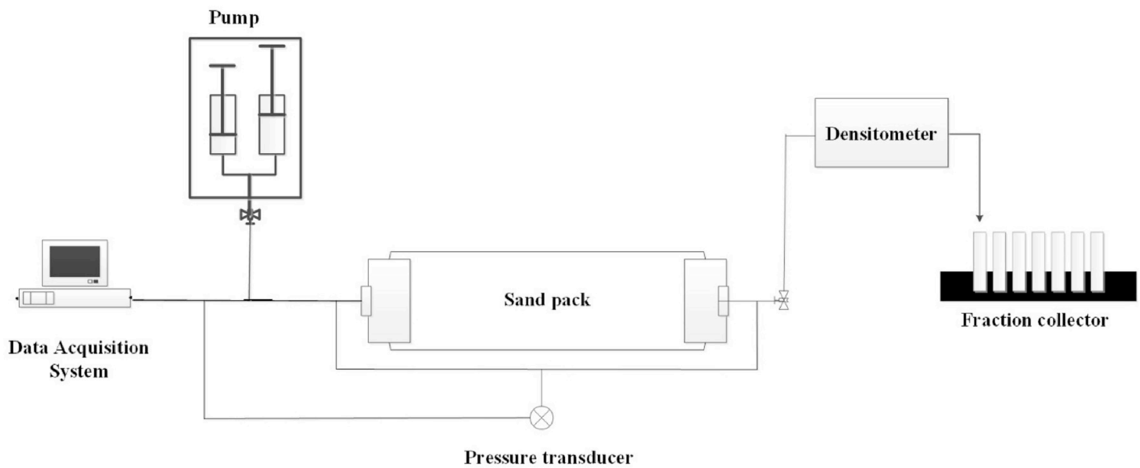

Fig. 3. Schematic of the core flooding experimental set-up.

Table 3
List of coreflooding experiments.

Oil type	Core flood test ID	Injection velocity (ft/d)	PV (mL)	OOIP (% PV)	BT[a] (min)	BT RF (% OOIP)	URF[b] (% OOIP)
Dodecane	50	0.1	22.23	79.42	2470.42	44.21	58.78
	32	0.7	22.17	78.8	503.72	48.16	64.02
	25	24.3	22.39	76.5	15.08	49.73	67.85
	49	121.5	22.11	79.73	3.40	58.00	70.22
	48	243	22.09	80.47	1.82	62.03	72.57
Mineral oil # 1	33	0.7	22.20	90.1	385.72	30.65	63.69
	24	24.3	22.02	87.9	11.65	34.79	68.06
Mineral oil # 2	37	0.7	22.07	86.75	391.42	29.54	55.92
	28	24.3	22.34	88.78	9.92	26.4	66.42
Mineral oil # 3	38	0.7	22.21	86.21	378.05	24.51	60.48
	30	24.3	22.22	85.78	8.20	20.42	54.03
Mineral oil # 4	40	0.7	22.34	85.76	277.92	17.06	54.34
	39	24.3	22.28	87.54	10.02	18.74	47.54
Heavy oil # 1	20	0.7	22.29	91.04	189.83	2.52	51.21
	23	24.3	22.08	91.06	9.78	3.21	39.05
Heavy oil # 2	11	0.7	22.23	92.53	224.62	1.17	25.34
	17	0.7	22.13	91.02	227.92	0.58	23.13
	10	24.3	22.33	91.62	6.03	0.38	10.37
	13	24.3	22.28	92.64	6.18	0.22	9.68

[a] BT = Breakthrough.
[b] URF = Ultimate recovery factor at 5 PV water injection.

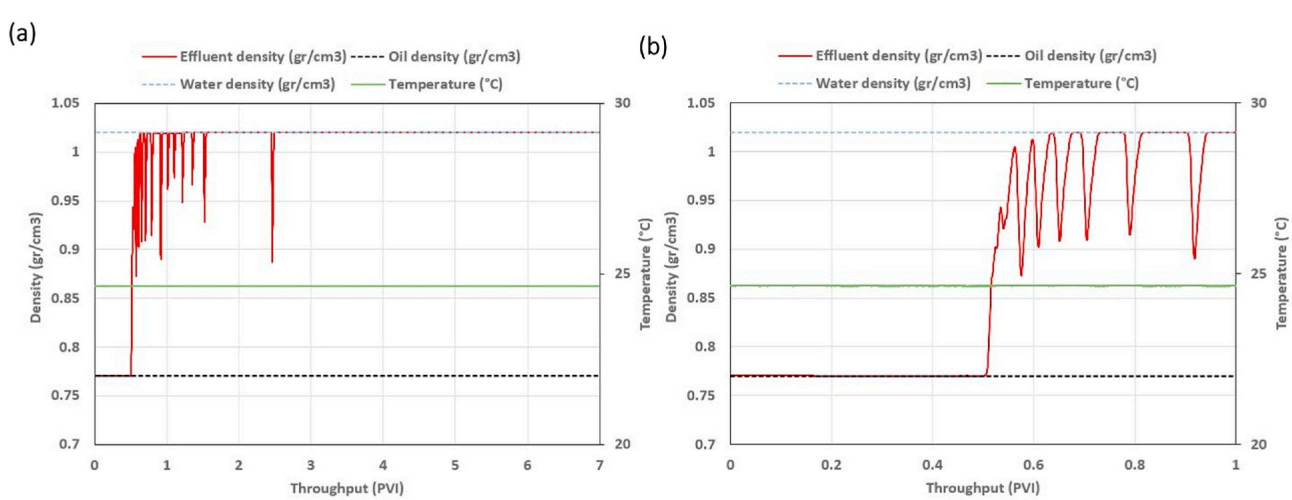

Fig. 4. Determination of breakthrough time based on in-line densitometer data: a) density profile obtained in test # 25 b) zoomed into the density profile to more clearly show the data over the first PVI (breakthrough time is 0.50 PVI or 15.08 min).

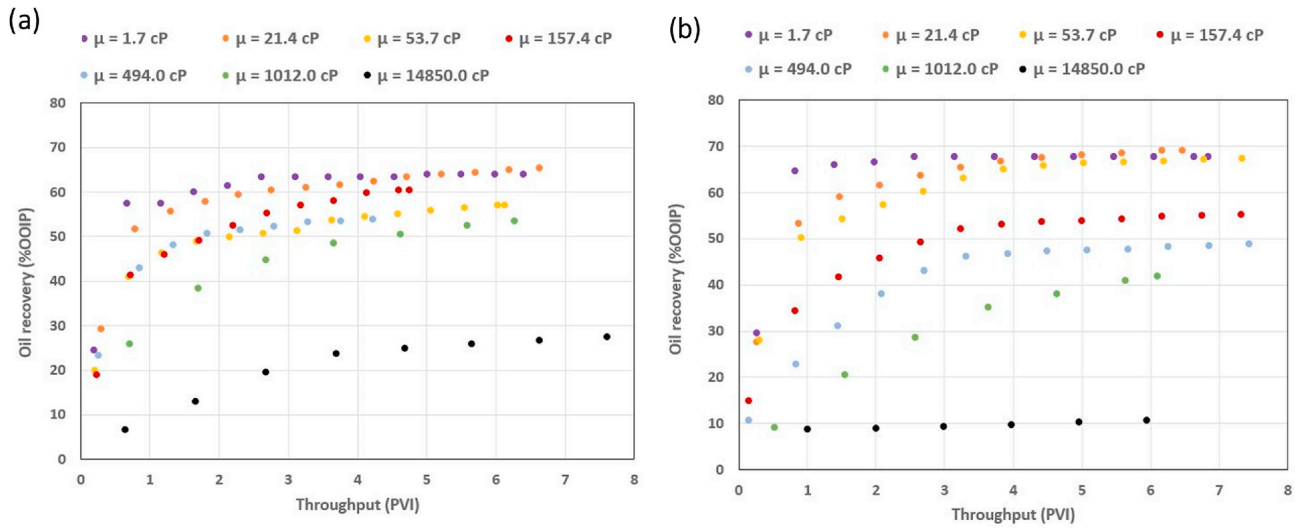

Fig. 5. Oil recovery vs. PVI for different oils in different floods at: a) 0.7 ft/D, b) 24.3 ft/D.

combined with the effect of capillary forces on oil recovery can explain the observed improvement in oil recovery with decreasing the velocity.

Viscous forces are reported to have a dominant effect up to the point of water breakthrough, so breakthrough oil recovery for different floods are presented in Fig. 7a. These breakthrough recoveries are determined through extrapolation of the recovery curves to the value exactly at the breakthrough time obtained from the in-line densitometer data, i.e., procedure explained in Fig. 4. Data presented in Fig. 7a suggest that with increasing oil viscosity there are three different flow regimes; at low oil viscosity (part A in Fig. 7a) breakthrough oil recovery increases with increasing injection velocity, at some moderate oil viscosity (part B in Fig. 7a) breakthrough oil recovery decreases with increasing injection velocity, and at high oil viscosity (part C in Fig. 7a) breakthrough oil recovery is almost independent of injection velocity and one single finger quickly dominates flow, which is called pseudo-stable flow. In the experiments with heavy oil # 2, pressure gradient across the core is built up before water breakthrough to 60 and 1790 psi in experiments # 11 (0.7 ft/D) and 10 (24.3 ft/D), respectively. The fact that despite this huge difference in pressure gradient breakthrough recovery is not only not higher in higher velocity flood but also a little bit lower (Table 3) suggests that viscous forces do not have a significant effect on oil production rate. Breakthrough oil recoveries in low velocity floods (tests 11 and 17) are very marginally higher than that of high velocity floods (tests 10 and 13) (Table 3), which may suggest the effect of imbibition even in early times. Also, to understand the late time flood behavior, the oil recovery beyond breakthrough i.e., oil recovery at 5 PVI excluding the recovery at breakthrough is also plotted in Fig. 7b. This condition can be considered as a conclusion stage of primary production, where continuous water pathways are already created within the reservoir. During this period, injected water mostly flows through the low resistance channels where there is low pressure gradient across the core.

Fig. 7b shows that at low oil viscosity there is almost no difference in oil recovery beyond breakthrough point. On the other hand, in high oil viscosity cases late time oil recovery is remarkably enhanced with decreasing injection velocity. This difference in late time oil recovery at low velocity floods compared to high velocity floods increases with increasing oil viscosity. This can be considered as a strong evidence proving the importance of capillary forces in heavy oil systems, as will be discussed later. This improvement in oil recovery with decreasing injection velocity at late times in heavy oil systems is consistent with literature (Mai et al., 2007; Newcombe et al., 1955) whose results are presented in Fig. 1a.

Breakthrough time, determined from the density data, for different floods are presented in Fig. 8. As expected, breakthrough time decreases with increasing oil viscosity; the more viscous the oil the more probable viscous fingering and in turn, the faster the water breakthrough.

To further revalidate the observations on the effect of velocity on oil recoveries, another core flood experiments with a sequential changing of injection velocity were done with dodecane (1.7 mPa s) and heavy oil # 2 (14,850.0 mPa s). As discussed, the results presented in Fig. 6 suggest that the balance between capillary and viscous forces is a function of oil viscosity; therefore, the lightest and the most viscous oils used in this study were chosen for these experiments to investigate the extreme cases and prove the discussed mechanisms for the oil recovery behavior.

4.1.1. *Effect of a sequential change in injection velocity on oil recovery*

Test # 10 was done with 14,850.0 mPa s oil and with injecting water at different injection velocities; 24.3 ft/D for the first 6 PVIs followed by 48.5, 97.0, 194.0, 388.1 ft/D for 1 PVI at each velocity, and finally 0.7 ft/D for around 4 PVI. As shown in Fig. 9a, oil recovery at the end of 6 PVI with velocity of 24.3 ft/D is 10.5% OOIP, which slightly increases to 12% OOIP with increasing velocity up to 388.08 ft/D at the end of 10 PVI (only 1.5% OOIP more oil produced during 4 pore volume injection of water at velocities of 48.5, 97.02, 194.04, 388.08 ft/D floods). However, as soon as the velocity is slowed down to 0.7 ft/D at 10 PVI oil recovery keeps increasing for the following two PVI i.e., 13.13% OOIP incremental oil recovery is obtained at the end of 12 PVI (Fig. 9a). These results are consistent with the data presented in Fig. 6g, where decreasing injection velocity from 24.3 to 0.7 ft/D results in a 15% OOIP incremental oil recovery. The pressure gradient across the core is also included in Fig. 9. As shown in Fig. 9a, pressure gradient keeps increasing to reach the maximum of 224 psi/ft at the end of injection at 388.08 ft/D. After slowing down the velocity to 0.7 ft/D, pressure gradient across the core sharply decreases to around 2 psi/ft at around 14 PVI. The combinations of oil recovery response and pressure gradient data suggest that the flow is not viscous-dominant where higher velocity with higher pressure gradient should result in a higher oil recovery which is not the case in Fig. 9a. At high velocity floods the injected water only passes through the water channels and does not touch the un-swept regions of the core surrounding the water channels. At low velocity flood, on the other hand, the injected water tends to imbibe into the smaller pores perpendicular to the water channels through capillary forces and displace the oil.

Fig. 9b shows the results of experiment # 50 where dodecane was used as the oil phase. In this experiment, water was injected at velocity of 0.1 ft/D for the first 6 PVIs followed by increasing velocity to 12.5, 24.3, 48.5, 97.02, 194.04, 388.08, 703.4 ft/D. The velocity was then reduced to 0.7 ft/D at 16 PVI, as shown in Fig. 9b. Oil recovery at the end

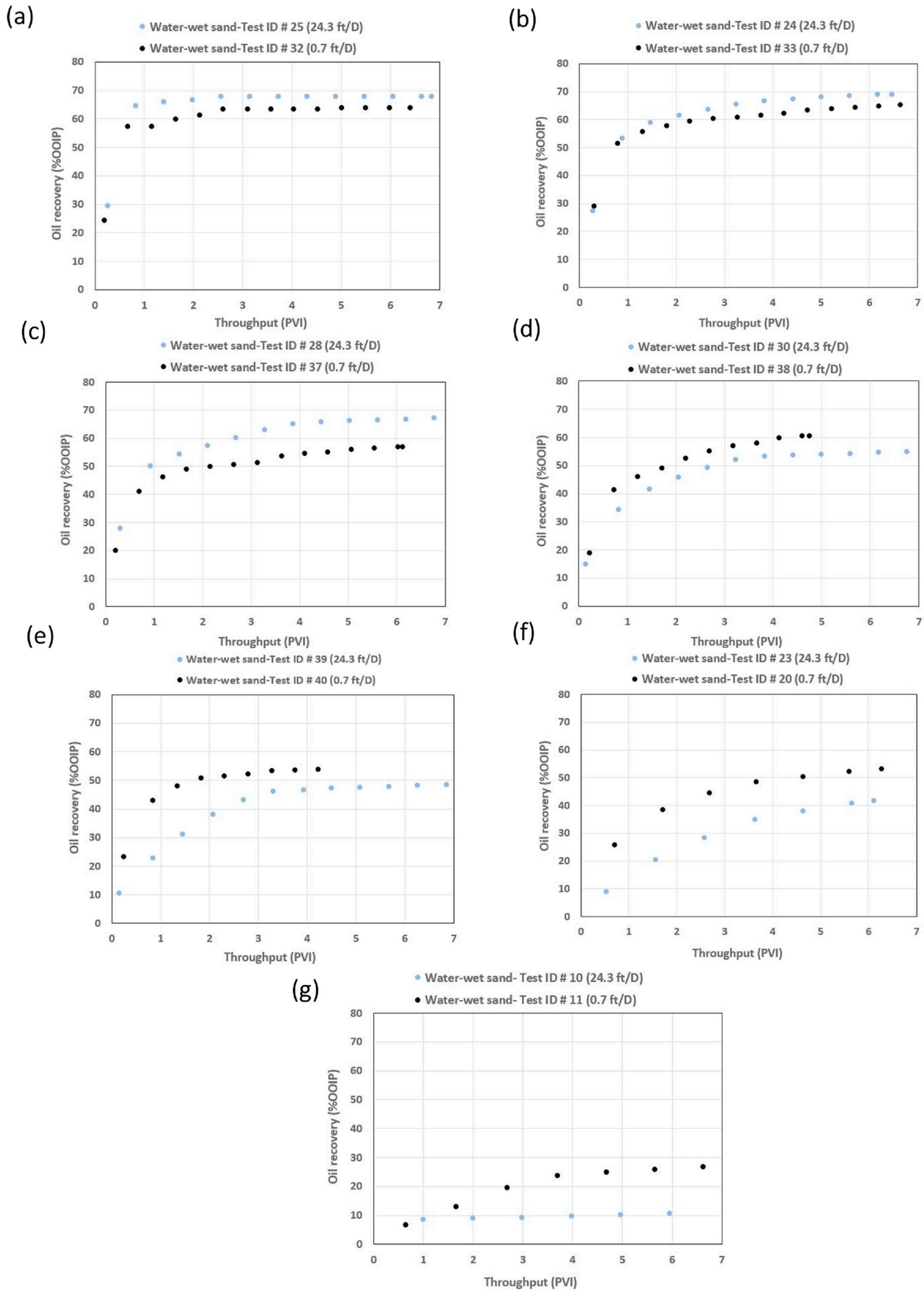

Fig. 6. Oil recovery at different injection velocities for different oils: a) dodecane (1.7 mPa s) b) mineral oil # 1 (21.4 mPa s) c) mineral oil # 2 (53.7 mPa s) d) mineral oil # 3 (157.4 mPa s) e) mineral oil # 4 (494.0 mPa s) f) heavy oil # 1 (1012.0 mPa s) g) heavy oil # 2 (14,850.0 mPa s).

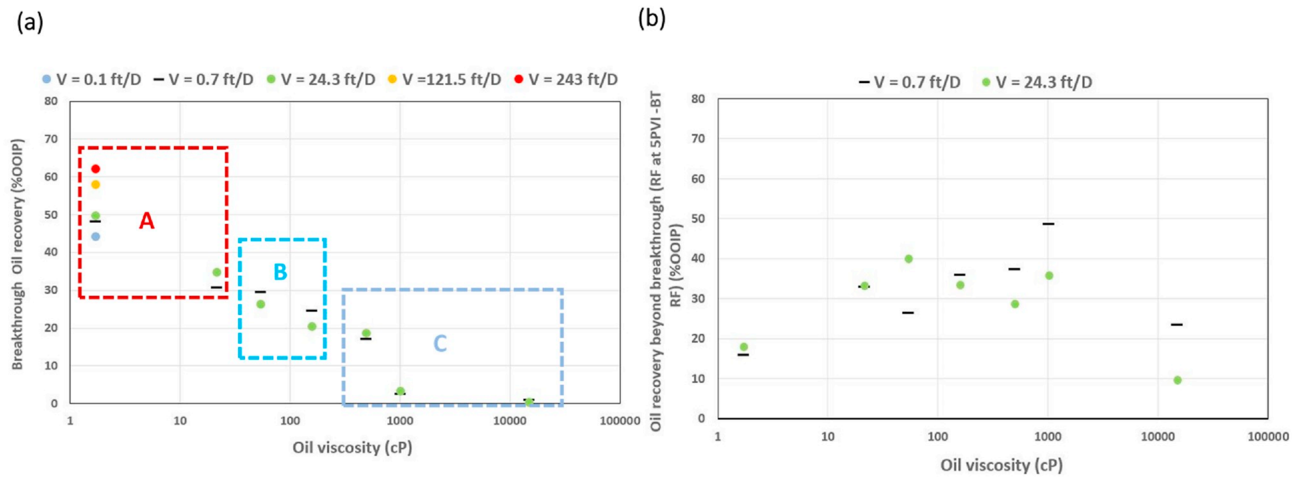

Fig. 7. a) Breakthrough oil recovery at different injection velocity vs. oil viscosity b) oil recovery at 5 PVI excluding breakthrough recovery.

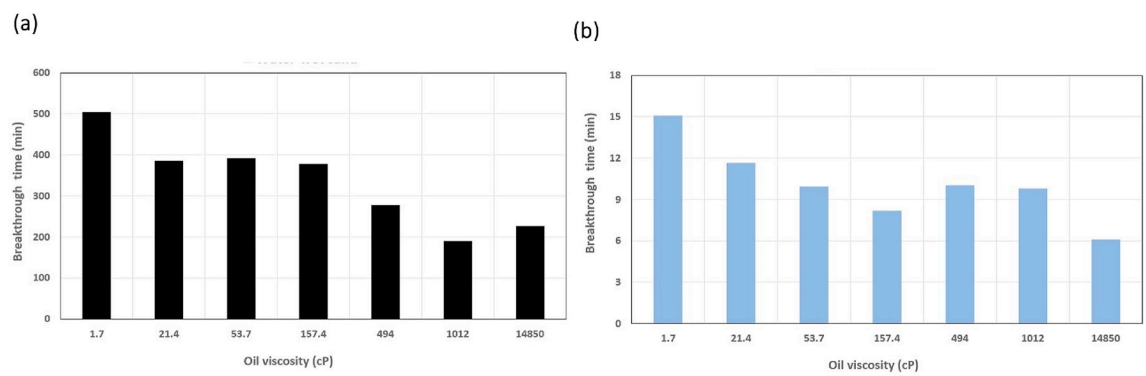

Fig. 8. Breakthrough time for different floods with different oils at: a) 0.7 ft/D, b) 24.3 ft/D.

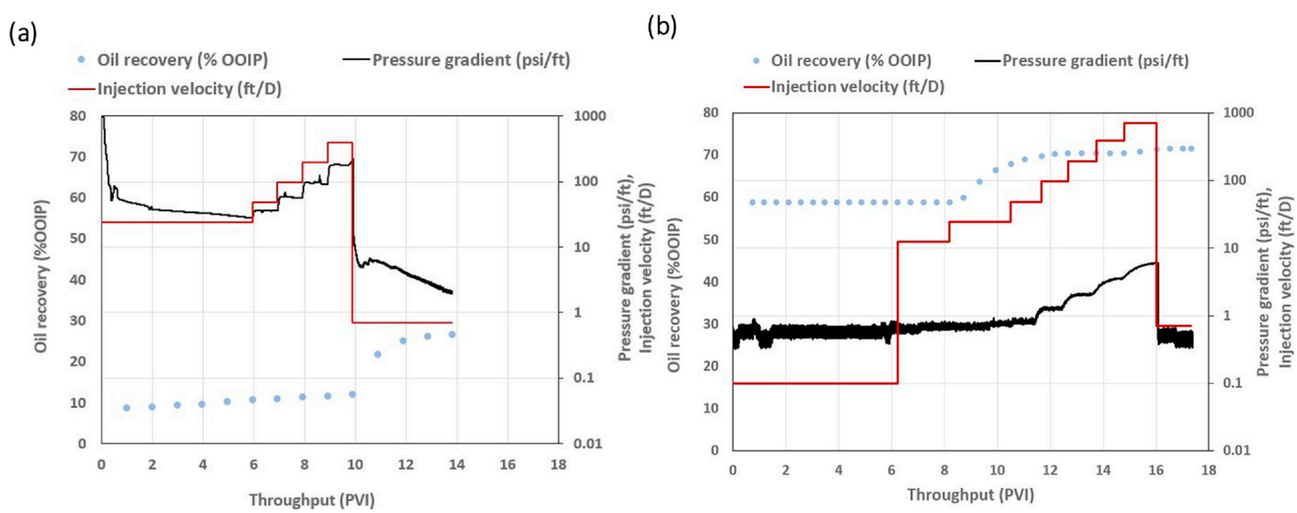

Fig. 9. Oi recovery, injection velocity, and pressure gradient across the core for a) test # 10 (oil viscosity = 14,850.0 mPa s) b) test # 50 (oil viscosity = 1.7 mPa s).

of 6 PVI at 0.1 ft/D is 58.8% OOIP. With increasing velocity to 12.5 ft/D for two more PVI (i.e., up to around 8 PVI) no more oil was produced. However, 9% OOIP incremental oil was produced upon increasing velocity from 12.5 to 24.3 ft/D at the end of 10.5 PVI. Further increase in injection velocity up to 703.4 ft/D did not result in any further noticeable oil recovery. Also, on the contrary to what observed with experiment with heavy oil # 2 (Fig. 9a), slowing down to 0.7 ft/D at 16 PVI did not result in any more oil recovery. One may argue that in this case the velocity was reduced to 0.7 ft/D at 16 PVI after 71.3% OOIP was already produced and the residual oil saturation was reached. However, oil recovery after 6 pore volumes injection of water at low velocity (0.1 ft/D) is 58.8% OOIP, which is much lower than that of the experiment # 32 (0.7 ft/D) and experiment # 25 (24.3 ft/D) with ultimate recovery at 5 PVI of 64.02 and 67.85% OOIP, respectively (Table 3). These results suggest that decreasing velocity does not lead to a better oil recovery for light oils, as opposed to heavy oils. The incremental oil recovery with increasing velocity from 12.5 to 24.3 ft/D indicates that the flow is viscous-dominant, which may not be supported with a further increase in injection velocity up to 703.4 ft/D. No further incremental oil recovery with further increasing velocity may be explained by the fact that in this experiment the water channel has been already created before further increasing velocity. So, some other experiments were performed where injection velocity was increased from the beginning to investigate the effect of increasing viscous forces before water breakthrough on oil recovery (Fig. 10).

As shown in Fig. 10a, increasing injection velocity to provide more viscous forces results in a more oil recovery. The higher maxima in the pressure gradient profile for the higher velocity floods (Fig. 10b) also support the more viscous forces before breakthrough. In a water-wet system, small to medium-sized pores are accessed through imbibition phenomenon and increasing injection velocity results in accessing larger pores, which are bypassed at slower floods. Beyond the point of water breakthrough, there is a sharp decrease in pressure gradient, indicating circulating water through the water channels and no more access to the un-swept parts of the core. Oil recovery at breakthrough vs. different injection velocity is plotted in Fig. 11.

As shown in Fig. 11, breakthrough oil recovery increases from 44.2 to 48.2% OOIP with increasing injection velocity from 0.1 to 0.7 ft/D. With a further increase in injection velocity to 24.3 ft/D breakthrough recovery slightly increases to 49.7% OOIP. With a further increase in injection velocity to 121.5 and 243.0 ft/D breakthrough recovery remarkably increases to 58.0 and 62.0% OOIP, respectively. These three oil recovery behaviors indicate that there are different mechanisms at different velocities for fluid flow in porous media.

To investigate the effect of capillary end effect to disturb the floods responses in Fig. 11, breakthrough oil recovery is plotted against the scaling coefficient presented by Rapoport and Leas (1953) (Fig. 12). The initial increase in recovery (part A in Fig. 12) could be due to capillary outlet end effect, which is dealt with increasing velocity from 0.1 to 0.7 ft/D. Part B in Fig. 12 shows stabilized flow where oil recovery is almost constant with a further increase in scaling coefficient beyond 1. Parts A and B are consistent with literature data for light oils (Fig. 2a) in terms of stabilizing flow when the Rapoport and Leas's (Rapoport and Leas, 1953) scaling coefficient is greater than 1. Part C in Fig. 12 shows a sharp increase in oil recovery with a further increase in the scaling coefficient resulted from increasing injection velocity. This effect should indicate the viscous-dominant flow because the capillary outlet end effect is already dealt with in Part A. One may argue that this effect could

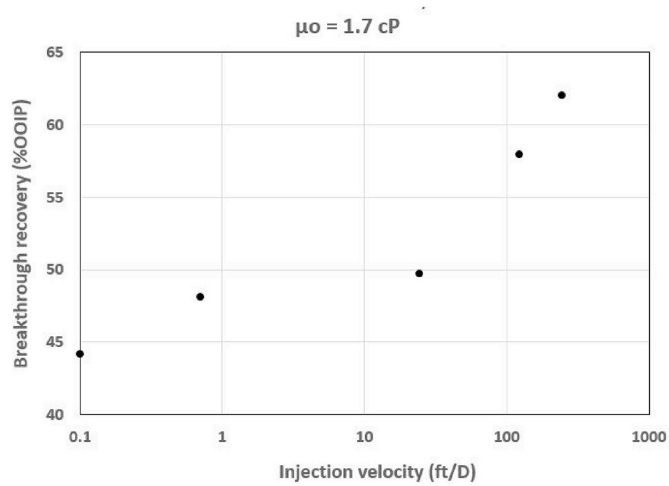

Fig. 11. Breakthrough recovery data vs. injection velocity (dodecane (1.7 mPa s) was used as the oil phase in these experiments).

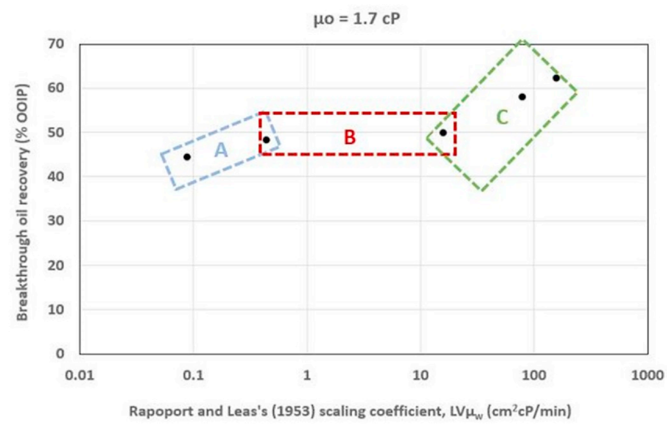

Fig. 12. Breakthrough oil recovery vs. Rapoport and Leas's (1953) scaling coefficient for the experiments done with dodecane and different velocities.

be attributed to the capillary inlet end effect which is reported at high injection velocities in strongly water-wet cores. However, capillary inlet end effect resulted from increasing injection velocity has been reported to decrease breakthrough oil recovery which is not the case in part C in

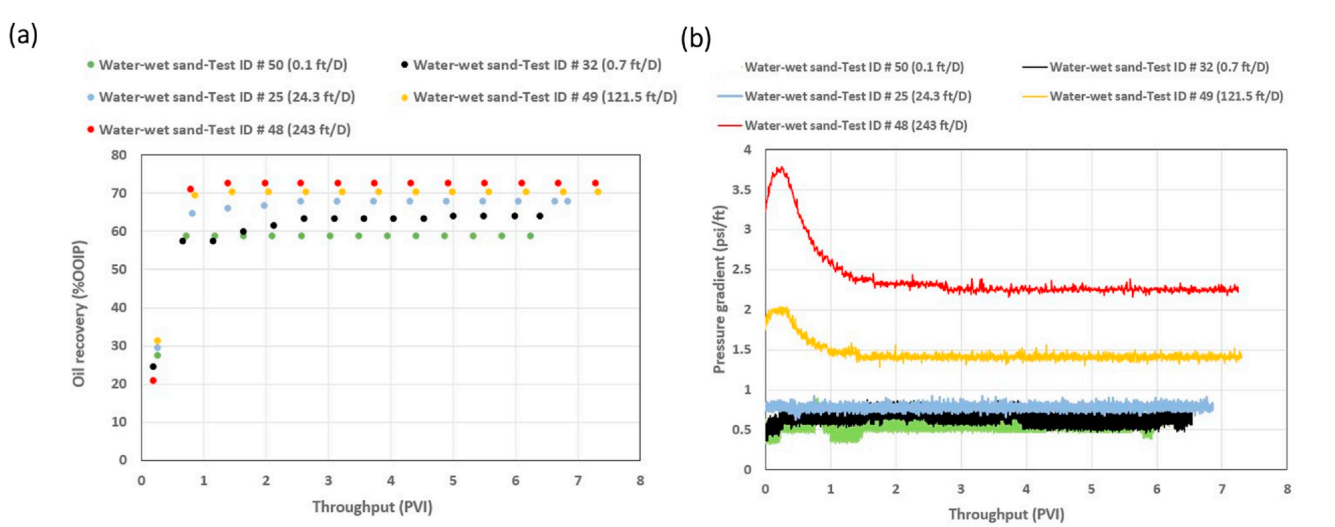

Fig. 10. Results of core floods with dodecane (viscosity = 1.7 mPa s) at different velocities a) oil recovery data b) pressure gradient across the core.

Fig. 12. Therefore, the recovery behavior observed in part C should not be due to capillary end effects and instead, indicates the viscous-dominant flow. As will be discussed later, the flood is still stable even at high velocities in part C in Fig. 12.

4.1.2. Repeatability of the experiments

Repeatability of experiments with the lightest (1.7 mPa s) and the most viscous (14,850.0 mPa s) oils used in this study are studied in Fig. 13. Final oil recovery at around 14 PVI in flood # 10 after flooding for around 4 PVI at 0.7 ft/D is 26.6% OOIP (Fig. 12a), which is very close to the final oil recovery of 27.5% OOIP at 8 PVI in flood # 11 with constant velocity of 0.7 ft/D. in addition, in flood # 25 with constant velocity of 24.3 ft/D the final recovery at around 7 PVI is 67.8% OOIP, which is very close to the oil recovery of 67.9% OOIP observed in flood # 50 at 10.5 PVI when the core was flooded for 2.5 PVI at 24.3 ft/D.

5. Data analysis

5.1. Scaling of imbibition

Different researchers tried to model capillary imbibition and correlate its rate with time and other governing parameters (Aronofsky et al., 1957; Mattax and Kyte, 1962; Rapoport, 1954; Reis, 1992; Reis and Cil, 1993). Imbibition-dominant oil recovery has been shown to be a linear function of square root of time (Blair, 1960; Fischer and Morrow, 2005; Fernø et al., 2013; Reis and Cil, 1993; Handy, 1959; Washburn, 1921). Imbibition rate is also a function of rock and fluid properties and decreases with increasing oil viscosity, increasing permeability (leading to reduce capillary forces), and time. However, Mai and Kantzas (2009) emphasized on the importance of imbibition at late times (after water breakthrough) even in heavy oil systems with viscosity up to 11,500 mPa s. Based on their results, at early times (before water breakthrough), oil (6500 mPa s) production rate is proportional to water injection rate for different injection velocities of 0.07, 0.35, and 1.04 ft/D, which indicates the viscous-dominant flow during this period (Mai and Kantzas, 2008). As time progresses beyond breakthrough the ratio of oil production rate to water injection rate is smaller and less stable in faster floods compared to the slower floods, leading to a decline in oil cut or an increase in water cut making the flood less efficient. The water cut in the slower flood also increases but to a smaller extent compared to the faster flood, indicating more chance for water to imbibe into the un-swept oil-saturated region of the core to displace the oil rather than just circulating through the water channel (Mai and Kantzas, 2008). Oil recovery normalized to the final oil recovery at 5 PVI vs. square root of time is plotted for different oils and different velocities (Fig. 14). Slope of oil recovery curves vs. square root of time is also plotted in Fig. 15.

As shown in Fig. 15, there is a monotonic decrease in the slope with increasing oil viscosity, which suggests that the flow regime is changing from viscous dominant in light oil systems to the imbibition-dominant flow in viscous oil systems. In addition, at the same oil viscosity, the slope is much higher in higher velocity floods compared to the lower velocity floods. This discrepancy in the value of slope in high velocity floods compared to the low velocity floods is more pronounced in lower oil viscosity cases where flow is viscous-dominant, and more velocity floods deliver more oil. On the other hand, with increasing oil viscosity since the flood is not stable anymore increasing velocity leads to viscous fingering and just circulating the injected water through the pre-formed channels with no more incremental oil recovery. This effect will be discussed later in instability analysis section.

Imbibition laboratory data has been tried to be scaled in terms of normalized oil recovery vs. dimensionless time. The first equation was proposed for imbibition of one phase of negligible viscosity into a tube (Lucas, 1918; Washburn, 1921), where imbibition rate is very quick at the beginning and then dramatically slows (Mason et al., 2010). To extend this concept to the two-phase flow in porous media, Rapoport (1954) combined capillary pressure definition, continuity equation, and Darcy's law. Rapoport's work was extended by Mattax and Kyte (1962) to define a dimensionless time as $t_{D\ \text{Mattax and Kyte,}\ 1962} = \frac{1}{L^2}\sqrt{\frac{K}{\varphi}}\frac{\sigma}{\mu_w}t$, where K, φ, σ, μ_W, L, and t are permeability, porosity, interfacial tension, water viscosity, and core length, respectively. This dimensionless group is a form of inverse capillary number and expresses the importance of capillary forces over viscous forces (Morrow and Mason, 2001), where $\sqrt{\frac{K}{\varphi}}$ is proportional to Leverett (1941) radius and reflects the effect of microscopic pore geometry on imbibition. This equation ignores the effect of oil viscosity, relative permeabilities, capillary pressure characteristics, core shape, and gravity. In a short, small diameter strongly water-wet core, gravity forces are very small compared to the capillary forces and so gravity effect can be safely neglected. To include the effect of oil viscosity, Ma et al. (1995), used different oils including n-decane, refined oils, white oil, and their mixture having various viscosity ranging from 0.92 to 156.31 mPa s and measured imbibition rate as a function of oil viscosity. They incorporated an empirical factor equal to geometric mean of oil and water viscosity ($\sqrt{\mu_o\mu_w}$) into the dimensionless time equation and presented the most widely used expression ($t_{D_{Ma\ et\ al.,\ 1995}} = \frac{1}{L^2}\sqrt{\frac{K}{\varphi}}\frac{\sigma}{\sqrt{\mu_o\mu_w}}t$) to correlate oil recovery rate vs. imbibition time. Zhang et al. (1996), replaced the core length in the dimensionless

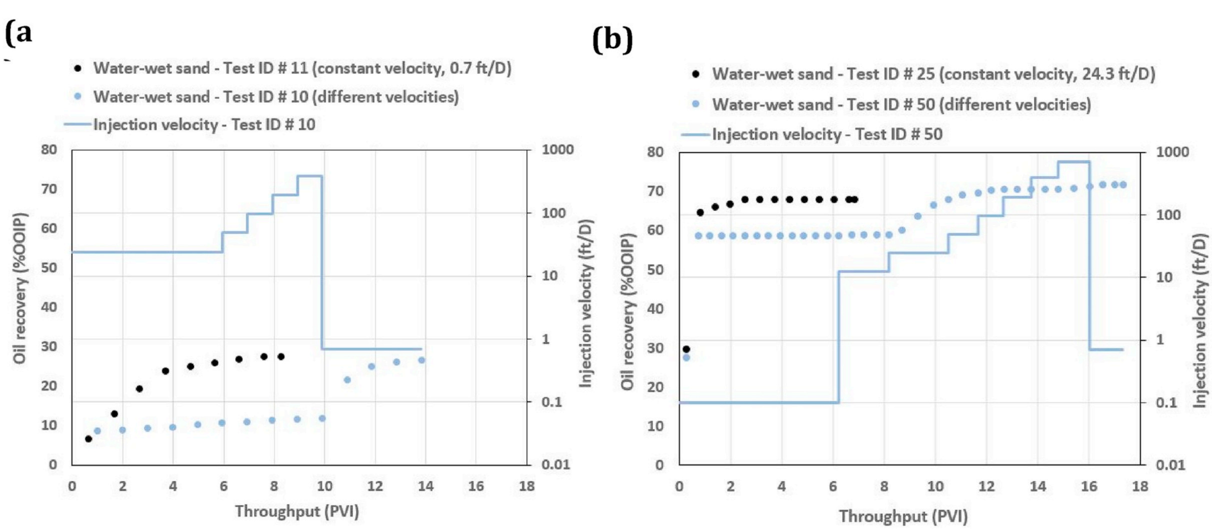

Fig. 13. Strong repeatability of experiments with a) heavy oil # 2 (14,850.0 mPa s) b) dodecane (1.7 mPa s), as the oil phases.

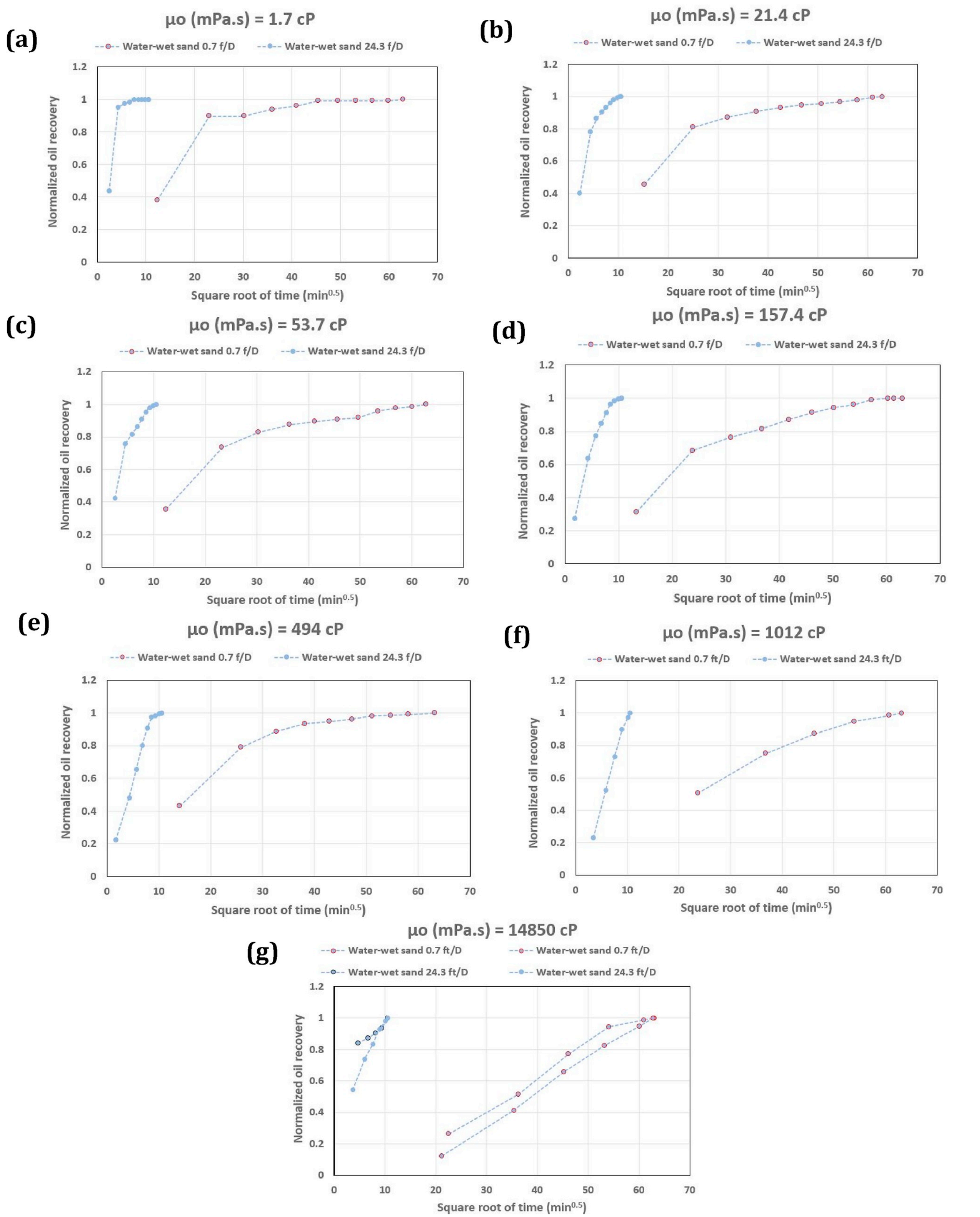

Fig. 14. Oil recovery normalized to the final oil recovery at 5 PVI vs. square root of time for different oils at different injection velocities: a) dodecane (1.7 mPa s) b) mineral oil # 1 (21.4 mPa s) c) mineral oil # 2 (53.7 mPa s) d) mineral oil # 3 (157.4 mPa s) e) mineral oil # 4 (494.0 mPa s) f) heavy oil # 1 (1012.0 mPa s) g) heavy oil # 2 (14,850.0 mPa s).

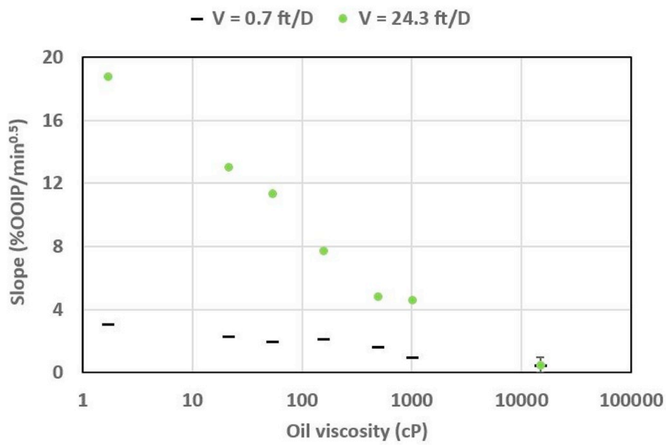

Fig. 15. Slope of oil recovery curve vs. square root of time for different oil viscosity.

time equation with characteristic length, L_c, to consider the combined effects of core shape and boundary conditions. In a systematic study, they used twelve cores cut from a block of Berea sandstone having various length from 1.17 to 10.24 cm with similar diameter of 3.81 cm. The cores were epoxy sealed in different ways to have various boundary conditions; only lateral surface of the core was open to imbibition (i.e., two core ends were epoxy sealed), only two ends were open to imbibition (i.e., the lateral surface was epoxy sealed), and only one end of the core was open to imbibition. They presented the characteristic length of $L_c = \frac{L}{2}$, where L is core length, for the system of two ends open to flow, which is the case in the core system used in this study. Mason et al. (2010), published an extensive review on the works aimed to incorporate a term considering oil viscosity into the dimensionless time (Fischer et al., 2008; Li and Horne, 2006; Reis and Cil, 1993; Ruth et al., 2004; Standnes, 2009; Wang, 1999; Zhou et al., 2002) and presented a modified term as ($\mu_w\left(1+\sqrt{\frac{\mu_o}{\mu_w}}\right)$) for viscosity term. They presented the following expression based on their experimental data for a wide range of oil to water viscosity ratio ranging from 0.008 to 173:

$$t_{D_{Mason\ et\ al.,\ 2010}} = \frac{2}{L_c^2}\sqrt{\frac{K}{\varphi}}\frac{\sigma}{\mu_w\left(1+\sqrt{\frac{\mu_o}{\mu_w}}\right)}t \qquad (1)$$

Mason et al. (2010) concluded that imbibition data can be correlated much better using the above correlation even without explicit relative permeabilities data compared to Ma et al. 's expression. They also claimed that this equation gives a better correlation compared to the expression derived from a standard two-phase flow theory based on optimized fixed value of relative permeability ratio. This expression was used to correlate normalized oil recovery data vs. dimensionless time (Fig. 16).

In the cases of low velocity floods (Fig. 16a), all the data, except the experiment with dodecane (1.7 mPa s viscosity), is correlated very well with dimensionless time. In these experiments, velocity is low enough (0.7 ft/D) and imbibition which is a slow process is the active mechanism. For high velocity floods (Fig. 16b), the data is correlated well with dimensionless time except for the two extreme oil viscosity cases i.e., experiment with dodecane (1.7 mPa s) and the experiments with heavy oil # 2 (14,850.0 mPa s). As mentioned before, at low viscosity the flow is recognized to be viscous-dominant; therefore, it is not unexpected if the data cannot be correlated with the correlation presented for imbibition-dominant flow. Also, in high velocity floods with heavy oil # 2 there is a severe viscous fingering, as will be discussed through instability analysis, with no chance for water to imbibe in a direction perpendicular to the direction of water channels. Therefore, in high velocity floods the flow is not imbibition-dominant and so oil recovery is not correlated with dimensionless time. Excluding these data i.e., the experiments with dodecane as the oil phase in both low (0.7 ft/D) and high (24.3 ft/D) velocity floods and the experiments with heavy oil # 2 (14,850.0 mPa s) at high velocity (24.3 ft/D) the other experiments' data are correlated well.

5.1.1. Field scale observations of imbibition

Optimal reservoir management in terms of adjusting voidage replacement ratio (VRR), defined as the ratio of water volume injected to the oil volume produced, is different in conventional light oil versus unconventional heavy oil reservoirs. In light oil reservoirs, the optimal strategy is to fully replace the voidage left after oil production with injecting water i.e., VRR = 1. In these reservoirs, a VRR <1 results in too much pressure decline leading to too much gas liberation. This high gas release leads to an increase in oil viscosity and very high gas mobility which in turn, makes oil production less efficient. Therefore, decreasing VRR decreases oil recovery in conventional light oil reservoirs. However, empirical evidence suggests that a VRR = 1 is not optimal in case of viscous heavy oil reservoirs (Vittoratos et al., 2014) and instead, a VRR < 1 leads to the most efficient water flood in these reservoirs. This condition can be achieved in practice with injecting water at a slower rate, which is translated to a more chance for water to imbibe into the un-swept oil-saturated portions of the reservoir leading to an improvement in oil recovery. Vittoratos et al. (2014), summarized the pros and

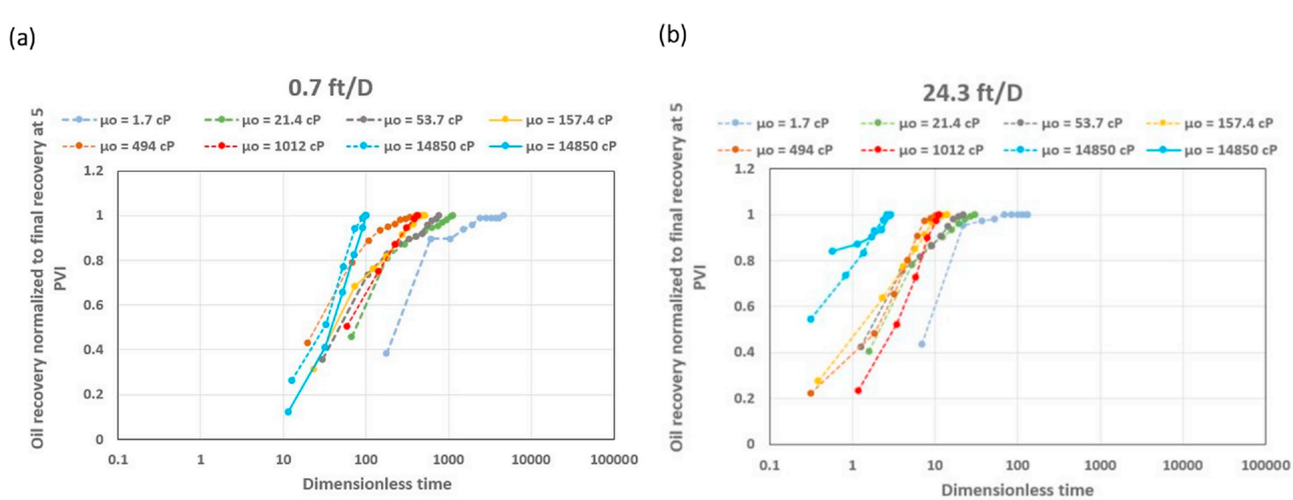

Fig. 16. Normalized oil recovery vs. dimensionless time for core flood experiments with different oils at a) 0.7 ft/D b) 24.3 ft/D.

cons of this reservoir management strategy. Based on their analysis, tuning a VRR <1 as opposed to VRR = 1 in heavy oil systems activates some mechanisms such as solution gas drive, foamy oil drive, emulsification, and three phase relative permeability interferences leading to enhance water flood performance. Solution gas drive and foamy oil drive (presence of liberated gas in oil) mechanisms lower gas mobility which in turn, lead to efficiently produce bypassed oil which is left behind due to viscous fingering. Lower gas mobility also slows down gas production which in turn, maintains reservoir energy in place. Increase in gas saturation also reduces relative permeability to water, which postpones water breakthrough. Another activated mechanism is emulsification due to the chemical changes during gas evolution. Water cut at the producer can be mitigated due to the emulsion flow in the "backbone" of the paths connecting an injector to a producer. They concluded that an increase in heavy oil viscosity due to gas liberation as pressure declines below bubble point may be compensated by the other activated mechanisms. They also performed a 1D simulation study and reported a significantly larger breakthrough oil recovery for VRR <1 compared to VRR = 1. However, total post-breakthrough oil recovery in case of VRR <1 is less than that of VRR = 1 on a time basis, while VRR <1 still recovers remarkably more oil than that of VRR = 1 for a given amount of water injected. They attributed this detrimental effect of VRR <1 on ultimate heavy oil recovery to the increase in oil viscosity due to pressure decline. They tried to adjust VRR <1 in their simulation study through either reducing water injection rate or increasing oil production rate. In another study on Wildmere and Wainwright pool water floods, Smith also pointed out that the excessive water injection should be avoided, i.e., voidage replacement ratio should be kept small, to prevent either flow of water into aquifer or driving oil out of the developed field boundaries (Smith, 1992). He also concluded that increasing water injection rate, which deteriorates sweep efficiency should be avoided in heavy oil systems. This conclusion is consistent with lab studies reported in Fig. 6f and g, which were done with heavy oil samples.

There are also other field studies discussing imbibition in heavy oil reservoirs. Husky investigated the effect of injector shut-in on the performance of reservoirs suspected for uneconomical water flood recovery (Adams, 1982). Adams (1982) reported a slight increase in oil production rate after shutting in the five water injectors in the South Aberfeldy Unit-Lloydminster area of western Canada. He also reported 40% decline in water cut and no noticeable increase in gas oil ratio (GOR) in the wells experienced shut-in. This shut-in assisted improvement in oil recovery has been also reported at lab scale (Mai and Kantzas, 2009). They reported an immediate increase in oil cut after reopening the core, which was shut-in after the initial 5 PV water injection. After shut-in period, whose duration was not specified in their article, water was injected at the same velocity as before shut-in (0.07 ft/D). They reported a change in slope of oil recovery after shut-in and attributed this improvement in oil recovery to the fluid redistribution during shut-in period, which leads to water imbibition into small-sized pores displacing oil into the larger pores or preformed channels already created after the first period of water injection. They made a conclusion that capillary forces and spontaneous imbibition can be significant even in very viscous oil (4650 mPa s) systems and in the absence of flow. Mai et al., also reported a slight decrease in water cut upon re-injecting water after soaking time (350 h) and the resultant increase in oil recovery (Mai et al., 2006). Based on their results, water cut immediately increases to catch up the same trend as before shut-in. So, it seems that lab scale studies support the field scale observations made by Adams (1982) regarding the increase in oil production rate after shut-in period.

5.2. Instability analysis

Instability analysis is a forces balance analysis, which describes that the displacement is unstable if the viscous forces are greater than the combination of gravity and capillary forces and the degree of instability increases with increasing injection velocity, keeping all other parameters constant. This is the case in water flooding of heavy oils, where the oil viscosity is much higher than that of water leading to an unstable displacement and low recovery factor. After water breakthrough, all the additional injected water will circulate through the low resistance preformed water pathways; therefore, instability analysis only explains oil recovery behavior up to breakthrough and not at late times (Mai and Kantzas, 2009).

Residual oil to water flooding in conventional light oil reservoirs is left behind as trapped blobs mainly due to capillary entrapment or due to bypassing resulted from reservoir heterogeneities (Chatzis et al., 1983; Moore and Slobod, 1955). However, at the end of heavy oil water flooding, residual oil is mainly left behind as bypassed oil due to the adverse mobility ratio between oil and injected water. In this case, there is an instability at the water front, where frontal perturbation starts to grow and becomes a viscous finger. This will result in premature water breakthrough and leaving a low resistance pathway through which the additional injected water will flow. This viscous fingering results in low breakthrough recovery since a considerable amount of oil in place is simply bypassed. Therefore, stability of displacing water front has been investigated to understand the relationship between breakthrough oil recovery and mobility ratio (water to oil mobility) (Peters and Flock, 1981; Bentsen, 1985). There are various versions of instability analysis (Bentsen, 1985; Sarma and Bentsen, 1987) in the literature; however, the work done by Peters and Flock (1981) is the basis of many studies (Bartley and Ruth, 2002; Dong et al., 2011; Mai and Kantzas, 2009; Maini et al., 1990; Peters and Khataniar, 1987; Sarma et al., 1990). Peters, (1979) was the first one who put forward the instability theory based on his core flood experimental data. The governing parameters like mobility ratio, displacement velocity, permeability, rock wettability, interfacial tension between displacing and displaced phases, and system dimensions were included in his analysis. Most of his core flood experiments were terminated at the time of water breakthrough beyond which the viscous fingering effect is not influential. Two types of cores were used; connate water bearing cores i.e., the vacuumed core was initially saturated with distilled water and non-connate water bearing cores, i.e., the vacuumed core was initially saturated with oil. He concluded that viscous fingering occurs in both water and oil-wet systems i.e., with and without connate water, respectively. He defined the following instability number to predict the onset of unstable displacement:

$$Ist = \frac{(M-1)v\mu_w D^2}{C^* \sigma K_{wor}} \quad (2)$$

where C^* is wettability index, which is reported to be 306.25 for strongly water-wet porous medium and 5.45 for oil-wet medium (Peters, 1979), M is end point mobility ratio $\left(\frac{K_{wor}\mu_o}{K_{oiw}\mu_w}\right)$, v is injection velocity, μ_w is water viscosity, D is the core diameter, σ is interfacial tension between oil and water, K_{wor} is end point permeability to water at residual oil saturation, and K_{oiw} is end point permeability to oil at irreducible water saturation. Peters and Flock (1981) emphasized the importance of wettability index in instability number equation. In strongly water-wet media, water imbibes into the small pores in the transverse direction delaying viscous fingering which is reflected by high values of C^* leading to low instability number. However, in oil-wet systems, there is no imbibition-assisted transverse flow (except at very slow injection rates) to delay viscous fingering and unstable displacement. In this case, since water flood is a drainage process water only flows through the largest pores (longitudinal flow) and not into the smaller ones (transverse flow) and so, the front cannot be stabilized.

Peters and Flock (1981) identified a critical value for the instability number equal to 13.56 below which the displacement is stable. Based on their results with water-wet sand, at low displacement rate the front is stable where breakthrough recovery is constant with increasing instability number, while at higher injection velocities the displacement is unstable i.e., breakthrough recovery is sharply declined with further increasing instability number. This sharp decline in breakthrough oil recovery was observed when $13.56 < I_{st} < 1000$. At this transition zone, they reported a poor reproducibility of the breakthrough recovery data for the water-wet system; therefore, they concluded that in this zone displacement is very sensitive to the core heterogeneities. At higher values of instability number ($I_{st} > 1000$), displacement is very unstable where flow is dominated by a single finger through which most of the injected water passes through. In this case, breakthrough oil recovery is very low and does not change with increasing instability number. In this case, the flow is called pseudo-stable, which is independent of injection velocity and instability number. Demetre et al. (1982), reported the onset of pseudo-stable flow at instability numbers greater than 900.

The results of 58 core flood experiments with water-wet sand, whose details are presented in Table 1, have been extracted from literature and used in instability analysis (Fig. 17). Wettability index is assumed to be 306.25, as suggested by Peters (1979). As seen in Fig. 17, there is a good power-law fit, with correlation coefficient of 0.721. Doorwar and Mohanty also tried to use the same equation as used in this study (equation (2)) to correlate breakthrough recovery with instability number (Doorwar and Mohanty, 2017). They used the same literature data as used in Fig. 17; however, they assumed wettability index of 1.0 for water-wet sand and reported a weak correlation coefficient of 0.529 for the power-law fit. The fact that the fit using equation (2) can be noticeably improved from 0.529 to 0.721, as shown in Fig. 17, with just incorporating wettability index value of 306.25 as suggested by Peters (1979) rather than just assuming 1.0 as is the case in Doorwar and Mohanty's work suggests the importance of wettability index. Therefore, we use the wettability index of 306.25 suggested for water-wet sand to calculate instability number.

Previous literature also used the same wettability index for the experiments with water-wet sand. In one study, Sarma et al. (1990), assumed that the silica sand used in their core flood experiments remained water-wet during the displacement experiments and so they assumed 306.25 as wettability index to calculate instability number. They used a non-polar mineral oil to exclude the effect of wettability alteration due to exposure of sand to the oil, which may justify their assumption about using the wettability index suggested for water-wet medium i.e., 306.25. In another study, Maini et al. (1990), also used the same number for the wettability index to calculate instability number in their system. They mentioned that they used the same rock and fluid system as used by Peters and Flock (1981), which justifies using the same wettability index. They also used non-polar mineral oil,

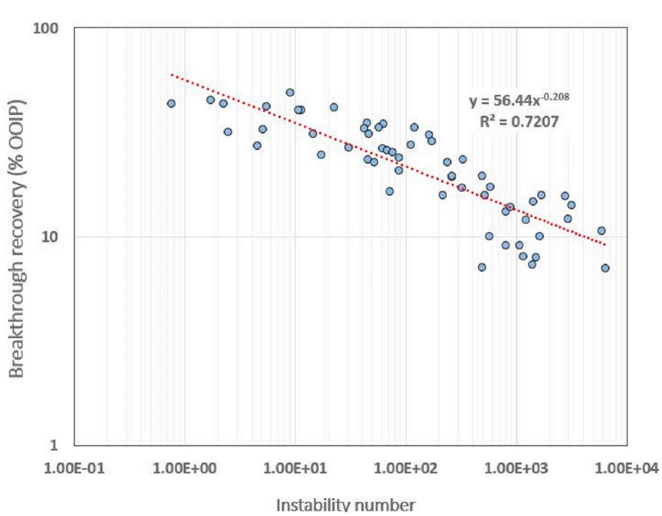

Fig. 17. Correlation between instability number and breakthrough recovery for 58 core flood experiments with water-wet sand (all the data are extracted from literature).

which may support the assumption of sand remaining water-wet during core flood experiments. Demetre et al. (1982), also used the wettability indices of 306.25 and 5.45 for the water-wet and oil-wet sand, respectively, as suggested by Peters and Flock (1981). They claimed that the first contacting fluid determines the wettability of the sand and considered the system water-wet when water was first used to saturate the core and oil-wet when silicone oil (Dow Corning 200) was first used to saturate the core. They never used a core twice to exclude the effect of silicone oil to gradually shift the wettability of sand from water-wet to oil-wet. In another study, Mai and Kantzas assumed wettability index of 306.25 (Mai and Kantzas, 2009) for their water-wet sand. They used two different heavy oils (4650 mPa s and 11,500 mPa s) in their study and assumed that sand remained water-wet even after exposure to the heavy oil. They used Lane Mountain 70 sand and performed water flood into the oil saturated core, which was left undisturbed for several days to reach equilibrium in terms of fluid distribution.

Fig. 18 shows breakthrough recovery vs. instability number for different oils and injection velocities. Some literature data are also included through dash data points. The displacement is stable at instability numbers below 13.56 i.e., no noticeable change in breakthrough recovery with increasing instability number, which is consistent with literature data. However, beyond the critical instability number there is a sharp decline in breakthrough recovery. This decline in breakthrough recovery is much sharper in the current study compared to the literature data included in Fig. 18. This could be due to the combined effect of very high oil viscosity and high injection velocities used in this study which justify very unstable flow. The most viscous oil in the literature data included in Fig. 18 is of 545.7 mPa s, which is much less viscous than the heavy oils used in this study.

As shown in Fig. 18, for the floods with dodecane (1.7 mPa s) as the oil phase, instability numbers are well below the critical value of 13.56 suggesting that the displacement is stable even for the flood with the highest injection velocity. Similarly, the displacement is stable (i.e., Ist < 13.56) for the flood experiments where oil viscosity is 21.4 mPa s (mineral oil # 1). In these stable floods, increasing viscous forces through increasing injection velocity results in more oil recovery at water breakthrough, as shown in part A in Fig. 7a. On the other extreme, for the experiments with the most viscous oil used in this study, i.e., heavy oil # 2 (14,850.0 mPa s), the displacement is unstable (i.e., Ist > 13.56) even at the lowest injection velocity i.e., 0.7 ft/D (Fig. 18). In these cases, breakthrough recovery is very low, as shown in Fig. 7a. This is the case for the displacement experiments at high injection velocity (24.3 ft/D) with heavy oil # 1 (1012.0 mPa s) and mineral oil # 4 (494.0 mPa s). In these cases, flow regime is pseudo-stable where breakthrough recovery is almost independent of injection velocity (part C in Fig. 7a). This flow regime occurs at instability numbers above 30 (Fig. 18), which is much less than the critical instability numbers previously reported for the onset of pseudo-stable flow; Demetre et al. (1982) reported a critical instability number of 900 for the onset of pseudo-stable flow, while Peters (1979) reported a critical instability number of 1000 for the onset of pseudo-stable flow. This discrepancy with literature could be attributed to the much higher oil viscosity in the current study compared to the Demetre et al.'s work where oil viscosity was 105.4 mPa s and Peters's work where oil viscosity was 102.0 mPa s. So pseudo-stable flow where one single finger grows very fast to dominate the flow occurs much sooner (at much less critical instability number). For the experiments with mineral oils # 2 and 3 with viscosities of 53.7 and 157.4 mPa s, respectively, instability analysis predicts that the foods are stable (Ist <13.5); however, increasing velocity in these two cases deliver less oil at breakthrough (part B in Fig. 7a). In these cases, slower floods deliver more oil at breakthrough, which suggests that imbibition activated at slower velocities plays a more important role in pushing oil out than that of viscous forces not only at late times (Fig. 7b) but also at water breakthrough (Fig. 7a). Good correlation of oil recovery data with dimensionless time, presented in Fig. 16a and b, supports the importance of imbibition in these floods.

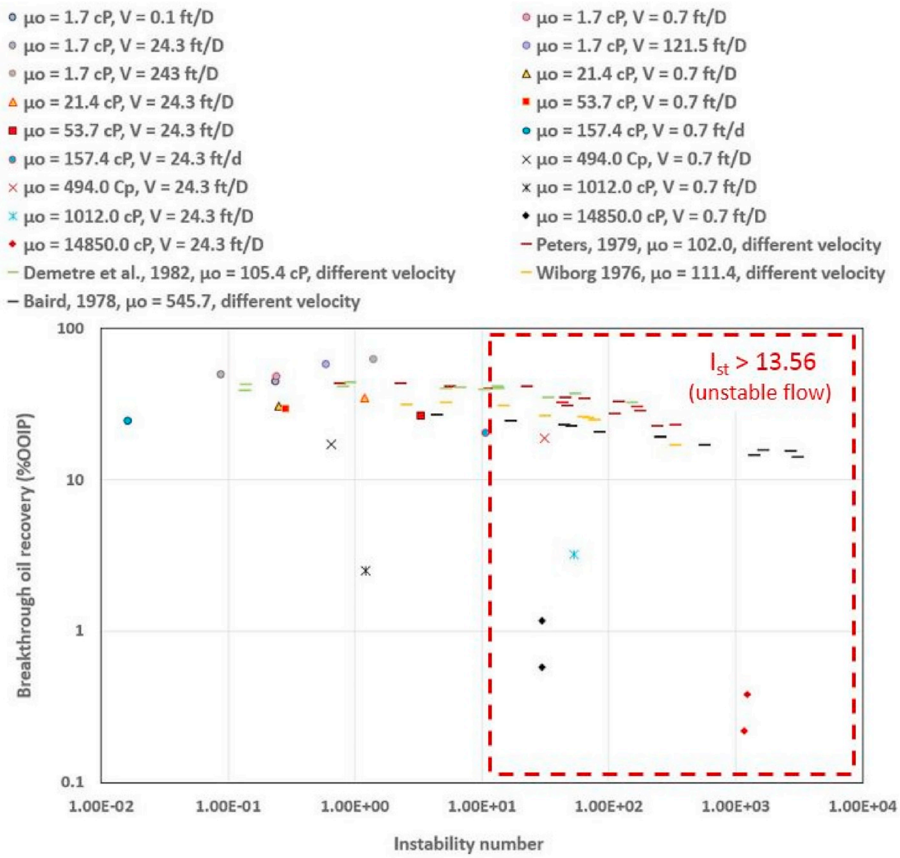

Fig. 18. Breakthrough oil recovery vs. instability number.

5.3. Interplay between imbibition and viscous forces

As mentioned, instability analysis is only applied to explain water flood behavior up to water breakthrough. Capillary number, however, may explain late time behavior of oil recovery in terms of ultimate residual oil saturation vs. the balance between viscous and capillary forces. The inherent assumption in light oil water flooding theory is that the oil-water viscosity ratio is assumed to be 1, based on which the capillary number is defined as $N_{Ca} = \frac{\mu_w V_w}{\sigma\ Cos\theta}$ (Moore and Slobod, 1956). In this equation, μ_w and V_w are the viscosity and velocity of displacing fluid, i.e., water in water flooding process, respectively, Θ is contact angle, and σ is interfacial tension between oil and water. This equation for capillary number was developed for light oil systems where there is no viscous fingering. The common understanding in light oil systems is that the oil displacement by water flooding is piston-like, which would be more uniform with increasing injection velocity (Mai and Kantzas, 2009). In water-wet systems, the smaller pores are preferentially accessed due to imbibition. In these cases, increasing an injection velocity increases viscous forces providing more chance to also access larger pores, where may not be accessible at smaller velocity floods. Therefore, increasing capillary number by either increasing injection velocity or decreasing interfacial tension decreases residual oil trapped by capillary forces.

In the presence of viscous fingers in water-wet heavy oil systems, on the other hand, either increasing injection velocity or decreasing interfacial tension both dampens imbibition leading to sever fingering and increase in bypassed oil saturation. In these cases, imbibition displaces water out of finger to stabilize the front. Therefore, capillary number equation should be modified to apply in viscous oil systems. Abrams, (1975) empirically introduced a viscosity ratio term into the capillary number equation as $N_{Ca} = \frac{\mu_w V_w}{\sigma\ Cos\theta}\left(\frac{\mu_w}{\mu_o}\right)^{0.4}$, which was based on the results of corefloods with different oils (0.4–37 mPa s). He also performed sensitivity analysis on the effect of relative permeability and pore structure. He found these parameters insignificant to improve correlation between residual oil saturation and dimensionless group expressing the ratio of viscous to capillary forces. The results of 178 core flood experiments from this study and literature were used to define a new capillary number (equation (3)). Different combinations of dimensionless groups were tested to incorporate the influence of oil to water viscosity ratio into the capillary number. The best fit to the experimental data was obtained through the following capillary number equation.

$$N_{Ca} = \left(\frac{\mu_w V_w}{\sigma\ Cos\theta\varphi}\right)^{0.26}\left(\frac{\mu_w}{\mu_o}\right)^{0.50}\left(\frac{K}{LD}\right)^{0.18} \tag{3}$$

In this equation, the effect of porosity is considered through actual velocity term ($\frac{V_w}{\varphi}$). The power for the water to oil viscosity ratio is obtained as 0.5 which is close to what Abrams, (1975) suggested, i.e., 0.4, for a limited range of oil viscosities. Core dimensions and absolute permeability are also included in this new scaling parameter. The correlation coefficient has been improved from 0.863 to 0.881 due to inclusion of permeability. With increasing permeability, as a measure of pore radius, capillary forces decrease, which is reflected in the modified capillary number through an increase in capillary number (the larger the modified capillary number the less significance of capillary forces compared to viscous forces). The core length and diameter were incorporated to make the term ($\frac{K}{LD}$) dimensionless. The combination of these modifications is the basis to extend the Abrams's equation (Abrams, 1975) for a much broader range of oil to water viscosity ratio. Fig. 19 compares the Abrams (1975) capillary number with the modified capillary number presented in this study (equation (3)). In both cases, the same experimental data with oil viscosity up to 15,000 mPa s were used. The data are more scattered with a correlation coefficient of 0.794

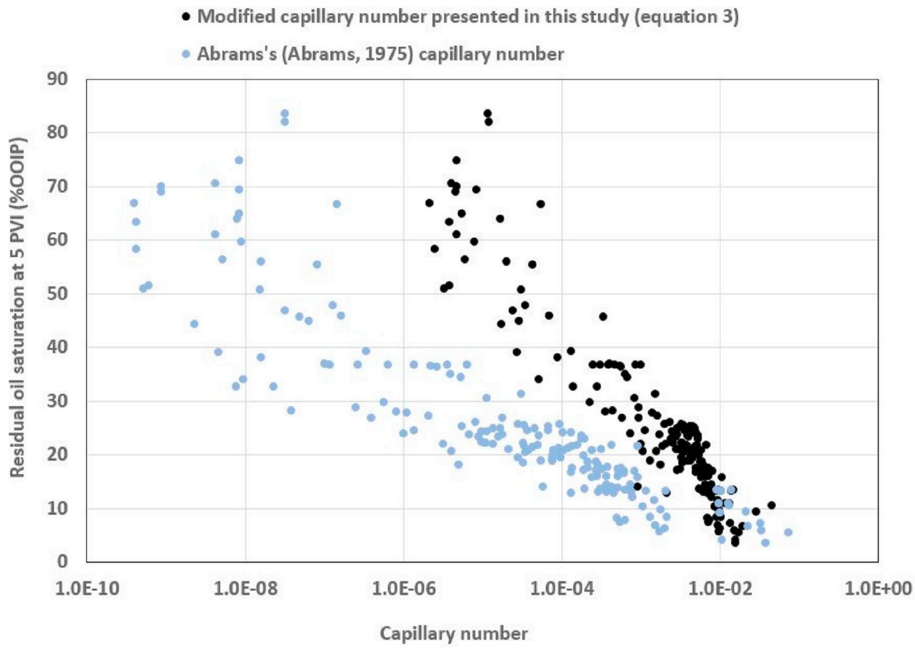

Fig. 19. Comparison of Abrams' (Abrams, 1975) capillary number with the modified capillary number (equation (3)) presented in this study (the same experimental data of 178 core flood experiments from this study and literature were used in both cases (oil viscosity is up to 15,000 mPa s)).

when plotted vs. Abrams' capillary number (which was suggested for oil viscosities in the range of 0.4 and 37 mPa s) compared to the case where the data are plotted vs. the modified capillary number (equation (3)) with a correlation coefficient of 0.881.

The new capillary number and instability number were used to map the interplay between capillary and viscous forces for corefloods of various injection velocities and different oils (Fig. 20). A, B, C, and D were identified as four different regions (Fig. 20). The floods with instability numbers below 13.56 (regions A and C in Fig. 20) are stable. In region A, capillary number is above a critical value of 10^{-4} (also reported by Abrams (1975) as a critical capillary number when oil viscosity is below 37 mPa s) so a further increase in capillary number through increasing injection velocity is the reason behind the velocity-assisted improvement in oil recovery (viscous-dominant flow) observed in Fig. 6a, b, and c. In region C, the floods are stable, but the capillary numbers are very low because either the velocity is very low

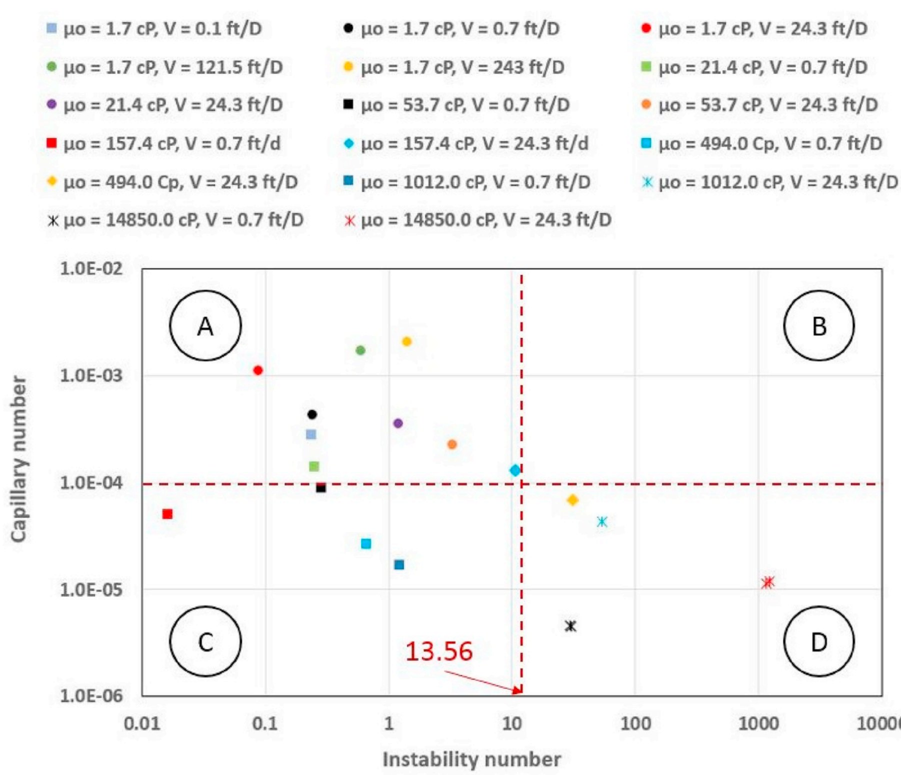

Fig. 20. Capillary number vs. instability number for different corefloods done with different oils at various velocities.

(0.7 ft/D in case of oil with 53.7 mPa s) or oil is very viscous. The floods mapped in region D are unstable (with instability numbers greater than 13.56) with capillary numbers below the critical value so there is no improvement in oil recovery with increasing capillary number and instead, oil recovery is increased with slowing down as shown in Fig. 6f and g. In experiments with the most viscous oil (14,850.0 mPa s), both low and high velocity floods are mapped in region D. In this region, instability numbers are very high indicating viscous fingering and capillary numbers are very low showing insignificant role of viscous forces. In these cases, imbibition activated at slower velocity is the main mechanism as quantified by the change in slope of oil recovery vs. square root of time shown in Fig. 14g. Regions A and D map the extreme cases of stable viscous-dominant flow and unstable imbibition-dominant flow, respectively.

6. Conclusions

Core flood experiments were conducted to understand the mechanisms responsible for water flooding of water-wet oil reservoirs. The balance between viscous and capillary forces and its effect on oil recovery were studied through changing injection velocity in experiments with seven oils with a broad range of oil viscosities from 1 to 15,000 mPa s at ambient temperature. Earlier work by Abrams (1975) showed that when oil viscosity is below 37 mPa s the product of capillary number and viscosity ratio $\frac{\mu_w V_w}{\sigma\ Cos\theta}\left(\frac{\mu_w}{\mu_o}\right)^{0.4}$ improves the correlation to residual oil saturation. Our observations show that water flood performance of viscous oils, with viscosity up to 15,000 mPa s, can be predicted through combination of Peters and Flock's (Peters and Flock, 1981) instability number and the modified capillary number, $N_{Ca} = \left(\frac{\mu_w V_w}{\sigma\ Cos\theta\varphi}\right)^{0.26}\left(\frac{\mu_w}{\mu_o}\right)^{0.50}\left(\frac{K}{LD}\right)^{0.18}$, presented in this study based on the results of 178 core floods. For stable floods (with instability numbers below a critical value), residual oil saturation decreases as capillary number increases, above a critical value of 10^{-4}, through increasing injection velocity. In viscous and unstable systems, on the other hand, capillary number is below a critical value since increasing velocity does not increase capillary number since the viscosity term $(\frac{\mu_w}{\mu_o})$ already reduced the capillary number. In these systems, increasing injection velocity promotes development of viscous fingers and increases residual oil saturation. In experiments with the most viscous oil used in this study (15,000 mPa s), the floods are unstable at both low and high velocities indicating the existence of viscous fingers in the system regardless of injection velocity. In these cases, there is no noticeable change in breakthrough oil recovery with slowing down the velocity; however, 14% OOIP incremental oil was recovered at late times with only reducing velocity. In viscous oil floods, the fact that even slow floods are unstable leaves imbibition as the only mechanism to improve late time oil recovery. So, it was concluded that optimizing injection velocity can remarkably affect the economics of water flooding projects. This optimized velocity is a strong function of oil viscosity.

Acknowledgement

Support for this research came from the Canada Excellence Research Chair program in Materials Engineering for Unconventional Reservoirs. The authors gratefully acknowledge the financial support of the FUR program from NSERC, AITF, and the sponsoring companies: Athabasca Oil Corporation, Devon Canada, Foundation CMG, Husky Energy, Brion Energy, Canadian Natural, Suncor Energy, as well as the Schulich School of Engineering (University of Calgary).

Appendix A. Supplementary data

Supplementary data to this article can be found online at https://doi.org/10.1016/j.petrol.2019.106691.

References

Alberta Energy and Utilities Board; 2001.
Adams, D.M., 1982. Experiences with waterflooding Lloydminster heavy-oil reservoirs. J. Pet. Technol. 34 (08), 1643–1650.
Anderson, W.G., 1987. Wettability literature survey-part 6: the effects of wettability on waterflooding. J. Pet. Technol. 39 (12), 1605–1622.
Abrams, A., 1975. The influence of fluid viscosity, interfacial tension, and flow velocity on residual oil saturation left by waterflood, SPE-5050-PA. SPE J. 15 (05), 437–447.
Aronofsky, J.S., Masse, L., Natanson, S.G., 1957. A model for the mechanism of oil recovery from the porous matrix due to water invasion in fractured reservoirs. In: SPE 932-G, Presented at 32nd Annual Fall Meeting of Society of Petroleum Engineers Held in Dallas. Texas, Oct. 6 - 9.
Bartley, J.T., Ruth, D.W., 2002. A look at break-through and end-point data from repeated water-flood experiments in glass bead-packs and sand-packs. In: SCA2002-17 Presented at the International Symposium of the Society of Core Analysts.
Batycky, J.P., McCaffery, F.G., Hodgins, P.K., Fisher, D.B., 1981. Interpreting relative permeability and wettability from unsteady-state displacement measurements. SPE J. 21 (03), 296–308.
Bentsen, R.G., 1985. A new approach to instability theory in porous media. SPE J. 25 (05), 765–779.
Blair, P.M., 1960. Calculation of oil displacement by countercurrent water imbibition. In: SPE 813 Presented at Fourth Biennial Secondary Recovery Symposium Held in Wichita Fails, May 2-3.
Bryan, J., Kantzas, A., 2008. Improved recovery potential in mature heavy oil fields by alkali-surfactant flooding. In: SPE 117649 Presented at the International Thermal Operations and Heavy Oil Symposium Held in Calgary, AB, 20-23 Oct.
Buckley, S.E., Leverett, M., 1942. Mechanism of fluid displacement in sands. Trans. AIME 146 (01), 107–116.
Buckley, J.S., Bousseau, C., Liu, Y., 1996. Wetting alteration by brine and crude oil: from contact angles to cores, SPE-30765-PA. SPE J. 1 (03), 341–350.
Chatzis, I., Morrow, N.R., Lim, H.T., 1983. Magnitude and detailed structure of residual oil saturation. SPE J. 23 (02), 311–326.
Craig, F.F., 1971. The Reservoir Engineering Aspects of Waterflooding. HL Doherty Memorial Fund of AIME, New York.
Demetre, G.P., Bentsen, R.G., Flock, D.L., 1982. A Multi-dimensional approach to scaled immiscible fluid displacement. PETSOC-82-04-05. J. Can. Pet. Technol. 21 (04), 49–61.
Dong, Y., Dindoruk, B., Ishizawa, C., Lewis, E.J., 2011. An experimental investigation of carbonated water flooding. In: SPE 145380 Presented at the SPE Annual Technical Conference and Exhibition Held in Denver, Colorado, U.S.A., October 30 – November 2.
Doorwar, S., Mohanty, K.K., 2017. Viscous-fingering function for unstable immiscible flows. SPE J. 22 (01), 19–31.
Emadi, A., Sohrabi, M., 2012. Mechanistic study of heavy oil recovery by waterflood: effect of oil viscosity and wettability. In: SCA2012-24 Presented at the International Symposium of the Society of Core Analysts Held in Aberdeen, Scotland, UK, 27-30 August.
Farouq Ali, S.M., 2006. Practical Heavy Oil Recovery.
Fernø, M.A., Haugen, Å., Wickramathilaka, S., Howard, J., Graue, A., Mason, G., Morrow, N.R., 2013. Magnetic resonance imaging of the development of fronts during spontaneous imbibition. J. Pet. Sci. Eng. 101, 1–11.
Fischer, H., Morrow, N.R., 2005. Spontaneous imbibition with matched liquid viscosities. In: SPE 96812 Presented at the SPE Annual Technical Conference and Exhibition, Held in Dallas, Texas, U.S.A., Oct. 9 – 12.
Fischer, H., Wo, S., Morrow, N.R., 2008. Modeling the effect of viscosity ratio on spontaneous imbibition. SPE Reserv. Eval. Eng. 11 (03), 577–589.
Handy, L.L., 1959. Determination of effective capillary pressures for porous media from imbibition data. In: SPE 1361-G Presented at Joint SPE-AIChE Meeting, May 19-20.
Holditch, S.A., 2013. Unconventional oil and gas resource development – let's do it right. J. Unconv. Oil Gas Resour. 1 (2), 2–8.
Jadhunandan, P.P., Morrow, N.R., 1995. Effect of wettability on waterflood recovery for crude-oil/Brine/Rock Systems. SPE-22597-PA. SPE Reserv. Eng. 10 (01), 40–46.
Kantzas, A., Brook, G., 2004. Preliminary laboratory evaluation of cold and post-cold production methods for heavy oil reservoirs part B: reservoir conditions. PETSOC-04-10-04. J. Can. Pet. Technol. 43 (10), 39–48.
Kennedy, H.T., Burja, E.O., Boykin, R.S., 1955. An investigation of the effects of wettability on oil recovery by water flooding. J. Phys. Chem. 59 (9), 867–869.
Koh, H., Lee, V.B., Pope, G.A., 2018. Experimental investigation of the effect of polymers on residual oil saturation. SPE-179683-PA. SPE J. 23 (01), 1–17.
Kyte, J.R., Rapoport, L.A., 1958. Linear waterflood behavior and end effects in water-wet porous media. J. Pet. Technol. 10 (10), 47–50.
Lake, L.W., Johns, R., Rossen, B., Pope, G., 2014. Fundamentals of Enhanced Oil Recovery, second ed. Society of Petroleum Engineers.
Leverett, M., 1941. Capillary behavior in porous solids. Trans. AIME 142 (01), 152–169.
Li, K.W., Horne, R.N., 2006. A general scaling method for spontaneous imbibition: an analytical model. SPE Reserv. Eval. Eng. 9 (03), 251–258.
Lucas, R., 1918. Ueber das Zeitgesetz des kapillaren Aufstiegs von Flüssigkeiten. Colloid Polym. Sci. 23 (1), 15–22.
Luo, P., Yang, C., Tharanivasan, A.K., Gu, Y., 2007. In Situ upgrading of heavy oil in a solvent-based heavy oil recovery process. J. Can. Pet. Technol. 46 (09), 37–43.
Lu, T., Li, Z., Li, S., Wang, P., Wang, Z., Liu, S., 2016. Enhanced heavy oil recovery after solution gas drive by water flooding. J. Pet. Sci. Eng. 137, 113–124.

Ma, S., Zhang, X., Morrow, N.R., 1995. Influence of fluid viscosity on mass transfer between rock matrix and fractures. In: Presented at the 46th Annual Technical Meeting of the Petroleum Society of CIM in Banff, Alberta, Canada, May 14 – 17.
Mai, A., Bryan, J., Goodarzi, N., Kantzas, A., 2006. Insights into non-thermal recovery of heavy oil. In: 2006-553 Presented at the 1st World Heavy Oil Conference.
Mai, A., 2008. Mechanisms of Heavy Oil Recovery by Waterflooding. PhD thesis. University of Calgary.
Mai, A., Bryan, J., Kantzas, A., 2007. Investigation into the mechanisms of heavy oil recovery by waterflooding and alkali-surfactant flooding. In: SCA2007-24 Presented at the International Symposium of the Society of Core Analysts, Held in Calgary, Canada, 10 – 12 September.
Mai, A., Kantzas, A., 2008. Improved heavy oil recovery by low rate waterflooding. In: SPE/PS/CHOA 117648 Prepared at the SPE International Thermal Operations and Heavy Oil Symposium Held in Calgary, Alberta, Canada, 20–23 October.
Mai, A., Kantzas, A., 2009. Heavy oil waterflooding: effects of flow rate and oil viscosity. J. Can. Pet. Technol. 48 (03), 42–51.
Maini, B., Coskuner, G., Jha, K., 1990. A comparison of steady-state and unsteady-state relative permeabilities of viscous oil and water in Ottawa sand. PETSOC-90-02-02. J. Can. Pet. Technol. 29 (02), 72–77.
Mason, G., Fischer, H., Morrow, N.R., Ruth, D.W., 2010. Correlation for the effect of fluid viscosities on counter-current spontaneous imbibition. J. Pet. Sci. Eng. 72 (1–2), 195–205.
Mattax, C.C., Kyte, J.R., 1962. Imbibition oil recovery from fractured, water-drive reservoir. SPE J. 2 (02), 177–184.
Mei, S., Bryan, J., Kantzas, A., 2012. Experimental study of the mechanisms in heavy oil waterflooding using etched glass micromodel. In: SPE-157998-MS Presented at the SPE Heavy Oil Conference Canada, 12-14 June.
Morrow, N.R., 1990. Wettability and its effect on oil recovery. J. Pet. Technol. 42 (12), 1476–1484.
Morrow, N.R., Mason, G., 2001. Recovery of oil by spontaneous imbibition. Curr. Opin. Colloid Interface Sci. 6 (4), 321–337.
Moore, T.F., Slobod, R.L., 1955. Displacement of oil by water-effect of wettability, rate, and viscosity on recovery. In: SPE-502-G Presented at the Fall Meeting of the Petroleum Branch of AIME, New Orleans, Louisiana, 2-5 October.
Moore, T.F., Slobod, R.L., 1956. The effect of viscosity and capillarity on the displacement of oil by water. Prod. Mon. 20, 20–30.
Morrow, N.R., Lim, H.T., Ward, J.S., 1986. Effect of crude-oil-induced wettability changes on oil recovery. SPE Form. Eval. 1 (01), 89–103.
Morrow, N.R., Ma, S., Zhou, X., Zhang, X., 1994. Characterization of wettability from spontaneous imbibition measurements. In: Presented at the 45th Annual Technical Meeting of the Petroleum Society of CIM Organized by the Petroleum Society of CIM, Co-sponsored by AOSTRA Held in Calgary, June 12-15.
Morrow, N.R., Tang, G., Valat, M., Xie, X., 1998. Prospects of improved oil recovery related to wettability and brine composition. J. Pet. Sci. Eng. 20 (3–4), 267–276.
Newcombe, J., McGhee, J., Rzasa, M.J., 1955. Wettability versus displacement in water flooding in unconsolidated sand columns. In: SPE 511-G Presented at Petroleum Branch Fall Meeting in New Orleans, Oct. 2– 5.
Olsen, D., 2018. Using a densitometer for quantitative determinations of fluid density and fluid volume in coreflooding experiments at reservoir conditions. Petrophysics 59 (01), 54–61.
Owolabi, O.O., Watson, R.W., 1993. Effects of rock-pore characteristics on oil recovery at breakthrough and ultimate oil recovery in water-wet sandstones. In: SPE 26935 Prepared at the Eastern Regional Conference & Exhibition Held in Pittsburgh, PA, U. S. 2-4 November.
Peters, E.J., 1979. Stability Theory and Viscous Fingering in Porous Media. PhD thesis. University of Alberta.
Peters, E.J., Flock, D.L., 1981. The Onset of instability during two-phase immiscible displacement in porous media. SPE J. 21 (2), 249–258.
Peters, E.J., Khataniar, S., 1987. The effect of instability on relative permeability curves obtained by the dynamic-displacement method. SPE Form. Eval. 2 (04), 469–474.
Rao, D.N., Girard, M., Sayegh, S.G., 1992. The influence of reservoir wettability on waterflood and miscible flood performance. J. Can. Pet. Technol. 31 (06), 47–55.
Rao, D.N., Girard, M., Sayegh, S.G., 1992. Impact of miscible flooding on wettability, relative permeability, and oil recovery. SPE Reserv. Eng. 7 (02), 204–212.
Rapoport, L.A., 1954. Scaling laws for use in design and operation of water-oil flow models. In: SPE 415-G Presented at Petroleum Branch Fall Meeting in San Antonio, Oct. 17-20.
Rapoport, L.A., Leas, W.J., 1953. Properties of linear waterfloods. J. Pet. Technol. 5 (05), 139–148.
Rathmell, J.J., Braun, P.H., Perkins, T.K., 1973. Reservoir waterflood residual oil saturation from laboratory tests. J. Pet. Technol. 25 (02), 175–185.
Reis, J.C., 1992. An analysis of oil expulsion mechanisms from matrix blocks during steam injection in naturally fractured reservoir. in-situ, 16 (1), 43–73.
Reis, J.C., Cil, M., 1993. A model for oil expulsion by counter-current water imbibition in rocks: one-dimensional geometry. J. Pet. Sci. Eng. 10 (2), 97–107.
Rodriguez, A.M.B., Binks, B.P., Sekine, T., 2016. Novel stabilisation of emulsions by soft particles: polyelectrolyte complexes. Faraday Discuss. 191, 255–285.
Ruth, D.W., Mason, G., Morrow, N., Li, Y., 2004. The effect of fluid viscosities on countercurrent spontaneous imbibition. In: SCA2004-11 Presented at the Society of Core Analysts Symposium, Abu Dhabi, October.
Salathiel, R.A., 1973. Oil recovery by surface film drainage in mixed-wettability rocks. J. Pet. Technol. 25 (10), 1216–1224.
Sarma, H.K., Bentsen, R.G., 1987. An experimental verification of a modified instability theory for immiscible displacements in porous media. J. Can. Pet. Technol. 26 (04), 88–99.
Sarma, H.K., Maini, B.B., Allen, G., 1990. Effects of viscous instability on unsteady-state relative permeability. In: CIMISPE 90-66 Presented at the International Annual Technical Meeting. Petroleum Society of Canada, June 10-13.
Skauge, A., Sørvik, A., Vik, B., Spildo, K., 2006. Effect of wettability on oil recovery from carbonate material representing different pore classes. In: SCA2006-01 Presented at the International Symposium of the Society of Core Analysts Held in Trondheim, Norway, 12-16 September.
Smith, G.E., 1992. Waterflooding heavy oils. In: SPE 24367 Presented at the SPE Rocky Mountain Regional Meeting Held in Casper, Wyoming, May 18–21.
Standnes, D.C., 2009. Calculation of viscosity scaling groups for spontaneous imbibition of water using average diffusivity coefficients. Energy Fuels 23 (4), 2149–2156.
Symonds, R.W.P., Farouq Ali, S.M., Thomas, S.A.R.A., 1991. A laboratory study of caustic flooding for two Alberta crude oils. J. Can. Pet. Technol. 30 (01).
Vittoratos, E.S., Zhu, Z., West, C.C., 2014. November). Optimal waterflood voidage management significantly increases oil recovery with minimal incremental cost. In: SPE 171937 Presented at the Abu Dhabi International Petroleum Exhibition and Conference Held in Abu Dhabi, U. A. E., Nov. 10 – 13.
Willhite, G.P., 1986. Waterflooding. Society of Petroleum Engineers.
Wang, J., Dong, M., Asghari, K., 2006. Effect of oil viscosity on heavy oil-water relative permeability curves. In: SPE 99763 Presented at the SPE/DOE Symposium on Improved Oil Recovery, Tulsa, Oklahoma, USA, 22-26 April.
Wardlaw, N.C., 1980. The effect of pore structure on displacement efficiency in reservoir rocks and in glass micromodels. In: SPE 8843 Resented at the First Joint SPE/DOE Symposium on Enhanced Oil Recovery Held in Tulsa, Oklahoma, April 20-23.
Wang, R., 1999. Gas Recovery from Porous Media by Spontaneous Imbibition of Liquid. MSc. Thesis. University of Wyoming, Laramie, Wyoming, USA.
Wardlaw, N.C., 1982. The effects of geometry, wettability, viscosity and interfacial tension on trapping in single pore-throat pairs. J. Can. Pet. Technol. 21 (3), 21–27.
Washburn, E.W., 1921. The dynamics of capillary flow. Phys. Rev. 17 (3), 273–283.
Zeppieri, S., Rodríguez, J., López de Ramos, A.L., 2001. Interfacial tension of alkane+ water systems. J. Chem. Eng. Data 46 (5), 1086–1088.
Zhang, X., Morrow, N.R., Ma, S., 1996. Experimental verification of a modified scaling group for spontaneous imbibition. SPE Reserv. Eng. 11 (04), 280–285.
Zhou, X., Morrow, N.R., Ma, S., 2000. Interrelationship of wettability, initial water saturation, aging time, and oil recovery by spontaneous imbibition and waterflooding. SPE J. 5 (02), 199–207.
Zhou, D., Jia, L., Kamath, J., Kovscek, A.R., 2002. Scaling of counter-current imbibition processes in low-permeability porous media. J. Pet. Sci. Eng. 33, 61–74.